University of Alberta
Printing Department

UNIVERSITY OF ALBERTA

EFFECT OF A MAGNETIC FIELD ON AGEING IN AL(RICH)-CU ALLOYS

A Thesis

Submitted to the Faculty of Graduate Studies
In Partial Fulfilment of the Requirements
for the Degree of Master of Science

DEPARTMENT OF MINING AND METALLURGY

by

EMILIO ALFREDO FALQUERO

EDMONTON, ALBERTA

OCTOBER, 1965

UNIVERSITY OF ALBERTA

FACULTY OF GRADUATE STUDIES

The undersigned certify that they have read and recommend to the Faculty of Graduate Studies for acceptance, a thesis titled

EFFECT OF A MAGNETIC FIELD ON

AGEING IN AL(RICH)-CU ALLOYS

submitted by EMILIO ALFREDO FALQUERO

in partial fulfilment of the requirements for the degree of Master of Science.

ABSTRACT

Al-Cu alloy specimens were aged in a magnetic field of 30 K. oersteds, and the ageing rates compared with those aged in the absence of the field in order to determine the possible effects of the magnetic field on the ageing process. Samples of different purities and composition, subjected to varying degrees of cold work were investigated. In all cases the ageing rates of field and no-field samples were found to be identical within the limits of experimental error. A theoretical discussion on the effects of a magnetic field on diffusion and nucleation rates indicates that the magnetic effects are too small to influence ageing either through the kinetic or thermodynamic parameters.

ACKNOWLEDGEMENTS

The author wishes to express his gratitude to Dr, W.V. Youdelis for his guidance and supervision during the course of this project. He is also indebted to Mr. J.R. Cahoon, M.Sc. and Mr. M.J. Bibby, M.Sc., for their helpful criticism and discussion and to Mr. R.M. Scott for his assistance in the photography. The author is also indebted to Professor E.O. Lilge for his departmental supervision. The assistance of Mrs. F. Klein who typed the manuscript is also greatly appreciated.

The financial assistance provided by a Canadian Commonwealth Scholarship is gratefully acknowledged.

TABLE OF CONTENTS

LIST OF TABLES

LIST OF FIGURES

INTRODUCTION

The modification and improvement of the mechanical properties of an alloy by the precipitation of an intermetallic phase from solid solution has received considerable attention since the turn of the century. The increasing industrial demand for engineering materials of greatly improved strength and hardness has lent great importance to this phenomenon, and the study of this phenomenon holds a significant position within the sphere of physical metallurgy. Of all the alloy systems characterized by solid solution precipitation, the Al-4%Cu alloy has received closest attention. The precipitation behaviour of this alloy proceeds through four distinct stages, exhibiting a variety of properties which can be helpful in the study of other precipitation systems. Furthermore, precipitation hardened Al-4%Cu alloy forms the basis of 'Duralumin', a popular engineering material showing considerable strength and hardness, yet being little heavier than pure aluminum.

The precipitation process is dependent mainly on nucleation and diffusion rates; it follows, therefore, that any variation in these rates would incur a change in the speed of precipitation. A theoretical treatment by Camp and Johnson[2] predicts small variations in the thermodynamic and transport properties of metals due to the presence of a magnetic field, and a recent investigation has shown that a field may cause a measurable inhibition in diffusion rates.[3,4] Moreover, a chemical or physical change of an alloy is usually accompanied by a change in magnetic susceptibility and this would give rise to an energy component if the change occurred in a magnetic field. Since the nucleation rate is exponentially dependent on energy, it is reasonable to assume that the

magnetic energy arising from a phase change in a field could influence the rate of nucleation and hence the rate of precipitation.

The possibility of a magnetic field affecting precipitation rates cannot be discarded even for systems where predictions based on classical diffusion and nucleation theory indicate that the magnetic effects would be negligibly small. It is a well known fact that physical reactions will often follow 'short cut' routes. Thus, in Al-Cu alloys the experimental activation energy for precipitation is considerably less than that predicted on the basis of known activation energies for volume diffusion, and it is suspected that some diffusion occurs through dislocation fault lines and other defects.[5] Thus there exists a possibility that a magnetic field could influence diffusion along the 'short cut' routes as well as the normal lattice diffusion.

The purpose of this investigation is to determine what effects, if any, a moderately strong magnetic field has on the precipitation rate of an age-hardening Al-4%Cu alloy. Apart from a purely academic point of view, this has interest on a practical level as well, particularly the possibility of accelerated or decelerated precipitation rates altering the mechanical properties of structural members of age hardening alloys exposed to magnetic fields. Should nucleation and diffusion rates in Al(rich)-Cu be affected by a magnetic field, then identical specimens aged in and out of the field at the same temperature would exhibit different ageing rates. It is on this criterion that the present investigation of magnetic effects on precipitation rates is based.

LITERATURE REVIEW

I(a) PRECIPITATION HARDENING

The basic requirement for a precipitation hardening system is that the solubility limit should decrease with decreasing temperature. Figure 1 shows an alloy of composition C which exists in the homogeneous α solid solution at a temperature T_1. When the alloy is slowly cooled to T_2 it becomes super-saturated with respect to component B, and as a result a B-rich β-phase precipitates out of solution. However, when the alloy is rapidly quenched from a single phase solid solution to a low temperature, the precipitation of the β-phase is suppressed, and the alloy exists as an unstable super-saturated solid solution. The super-saturated alloy is in a metastable state, and on raising the temperature a moderate amount of β-phase will form and precipitate out of solution. This latter process differs from the former in that the precipitation is controlled to give a uniformly dispersed, specifically oriented precipitate which markedly increased the alloy's strength. It is known as an "age hardening" process and may be accelerated by the introduction of herterogeneous nucleating points or by raising the ageing temperature to increase diffusion rates.

X-Ray diffraction and electron microscopy studies have shown that the initial precipitate is seldom the same as the equilibrium phase. The ageing process generally follows a specific sequence: solid solution → zones → intermediate precipitate → equilibrium precipitate. However, under particular experimental conditions some of the phases may be avoided, i.e. although Al-4.5%Cu alloy follows the whole sequence when aged at 130°C (Figure 2), this alloy does not form G.P.(1) zones

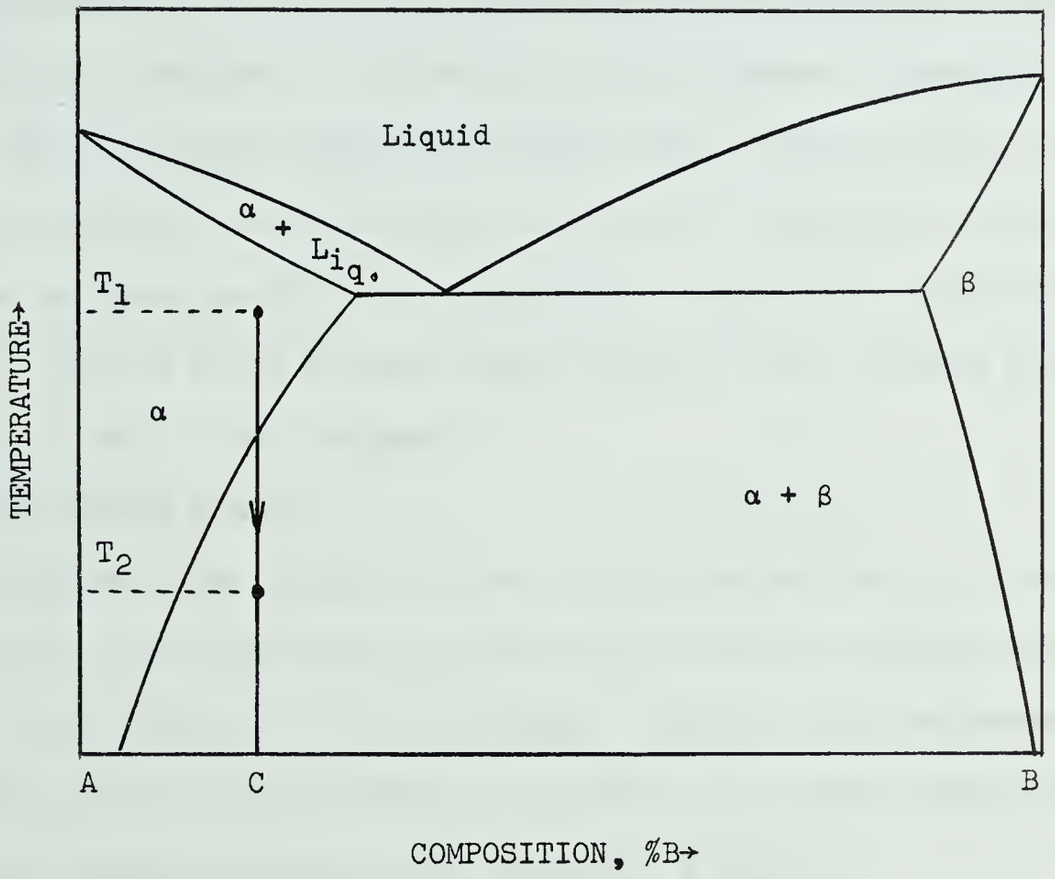

Figure 1. Equilibrium Diagram.

when aged at 190°C. The equilibrium precipitate is usually incoherent with the matrix, but the zones and intermediate precipitates are essentially coherent and form on particular crystallographic planes. Thus as precipitation proceeds the coherent lattice becomes increasingly strained since the atoms are subjected to inter-atomic forces due to the slight differences in lattice parameters existing between the precipitate and matrix lattices. This results in an increase in hardness, strength and electrical resistivity of the alloy. These reach a maximum for an optimum size of coherent precipitate, beyond which they decrease as continued growth of the precipitate destroys the coherency or registry. When an alloy is aged beyond the point where optimum strength exists it is said to be 'overaged'.

(b) PRECIPITATION STAGES

Aluminum-copper alloys of about 4.5% Cu content exhibit four distinct stages of precipitation when aged over a medium temperature range: G.P.(1)*, G.P.(2)* or θ", θ' and θ stages. In alloys aged at temperatures higher than 140°C and/or containing less than 4% Cu, one or more of the intermediate phases may be omitted (Figures 2 & 3).

The G.P.(1) zones are believed to be platelike clusters of copper segregated on the [100] planes of the aluminum-rich matrix. Such plates are small (100Å by 10Å) and thus remain coherent with the matrix. Continued precipitation of the alloy enlarges the plates thus generating lattice misfit strains and inducing hardness in the metal. When aged at room temperature the alloy never proceeds beyond the G.P.(1) stage, [9]

---

* G.P.indicate Guinier-Preston zones. These zones were discovered and studied simulataneously but independtly by Guinier[8] and Preston[7] about 1938.

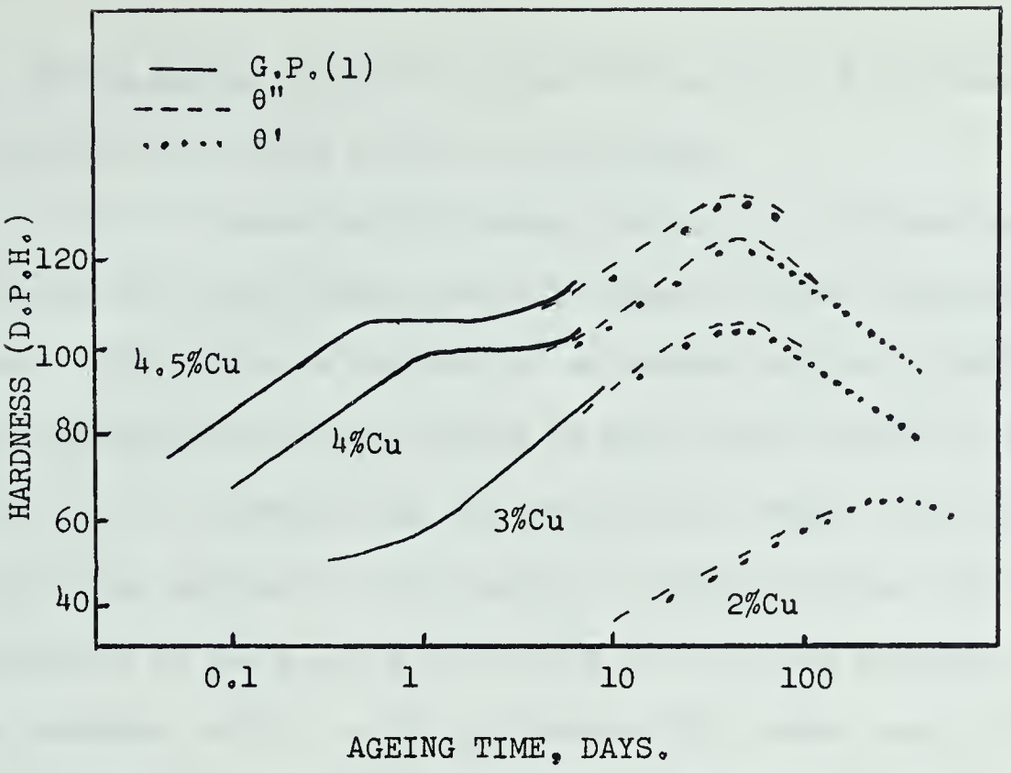

Figure 2. Hardness Vs. ageing-time curve at 130°C.[9] For Al-Cu alloys.

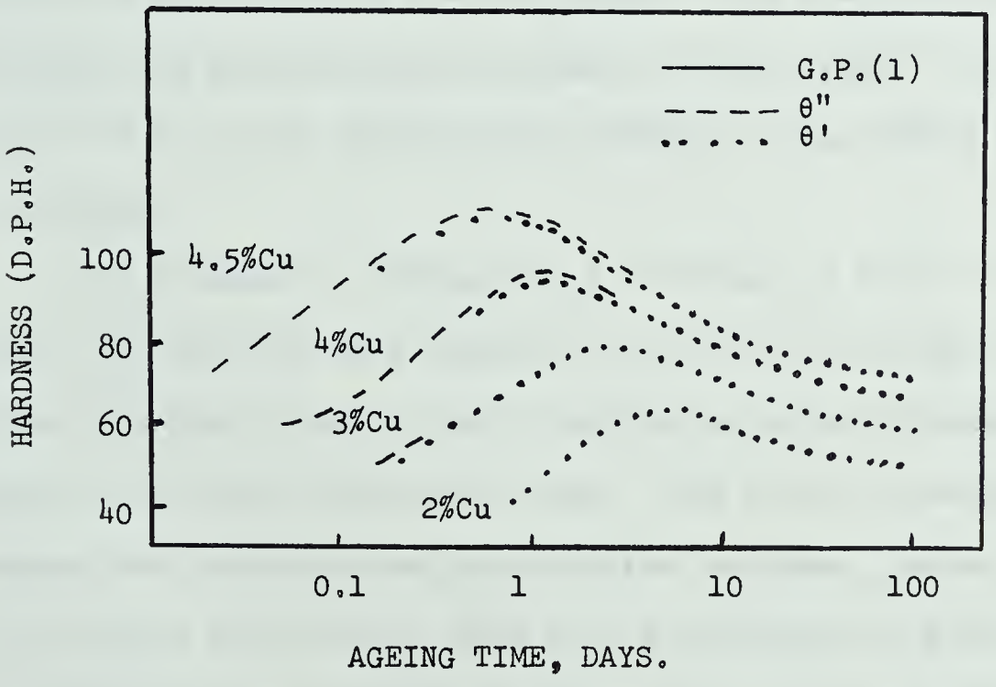

Figure 3. Hardness Vs. ageing-time curve at 190°C.[9] For Al-Cu alloys.

but during ageing at elevated temperatures the G.P.(1) zones are eventually superceded by the G.P.(2) zones.

G.P.(2) zones are not zones like G.P.(1) but quasi-coherent intermediate precipitates, and this stage is often designated as θ" phase. This phase is composed of an ordered crystal structure of average composition $CuAl_2$ and occurs in plates about 1500Å in diameter and 100Å thick. Although they are considerably larger than the G.P.(1) plates they maintain a high degree of coherency since the lattice parameters in the a and b directions fit into the aluminum lattice. The parameter misfit in the c direction will cause some lattice strains and this will become more pronounced as the size of the precipitated plates increases. Optimum hardness and strength conditions are usually associated with advanced θ"-phase growth. The θ"-phase eventually loses coherency and precipitation continues to the θ'-phase. The transition from θ" to θ' is not immediate and generally these phases overlap considerably.

The θ'-phase is tetragonal ($a = 4.04$Å, $c = 5.8$Å) in structure and forms with the main axis parallel to the $\langle 100 \rangle_{Al}$ direction. There is little coherency here and misfit strains are often released by the formation of stable dislocation loops. The lack of coherency, which becomes more pronounced as precipitation increased, causes a softening of the alloy; dislocations have little difficulty in moving through the unstrained lattice and the θ'-phase is usually associated with the overaged condition of the alloy.

The equilibrium precipitate, θ, is an intermetallic phase of composition $CuAl_2$. This phase is also tetragonal ($a = 6.06$, $c = 4.87$), but is completely incoherent with the matrix and its formation leads to

maximum softening. However, this phase only occurs after prolonged ageing at high temperatures and is seldom observed experimentally; Silcock et al[9] found traces of the θ-phase in 4% and 4.5% Cu alloys after ageing at 190°C for 100 days.

There exist some doubts as to whether the intermediate phases are formed by allotropic changes or nucleation from the matrix. Available evidence seems to suggest that either process may be valid. Silcock et al[9] showed that for certain conditions of composition and ageing temperature the precipitation could start at the θ" or θ' stage (see Figures 2 and 3). This indicates that θ" and θ' phases could be nucleated directly from the matrix. However, θ"-phase which is formed directly from the matrix has a c parameter of 7.6Å, yet when its formation is preceded by G.P.(1) zones the c parameter is invariably 8.0Å. The thickness of the θ' plates is also dependent on whether this phase is formed simultaneously with the θ"-phase. This evidence suggests that the formation of a certain phase may be dependent on the preceding phase.

It is probable that the main reaction is one involving nucleation and growth. However, a complete lack of allotropic change would imply that a given phase would dissolve into the matrix completely, prior to the formation of the subsequent phase; a concentration of copper would be completely dispersed only for a new concentration of copper to build up a macroscopic distance away. Such an unnecessary transfer of copper seems unreasonable. It is much more likely that a certain degree of allotropic change does take place. For example, a θ"-phase precipitate may dissolve partially until the remaining precipitate is sufficiently small for the atoms to be re-arranged into θ'-phase and then this would act as a nucleating point for further precipitation of θ'-phase.

II. THE MECHANISM OF PHASE CHANGE

A system which is in a supersaturated state, such as an alloy in which the solid solution state has been preserved by quenching, may lower its free energy by a change in structure or precipitation of a new phase. The mechanism leading to such a change may be explained with the aid of an "energy profile" and related theremodynamic concepts. Figure 4 illustrates the energy variations of an atom moving from an α-phase state to a β-phase state. It is apparent that to make the change $\alpha \rightarrow \beta$ the atom will need to acquire an activation energy of Q_1. The probability that all the atoms will simultaneously acquire this energy is remote and the reaction does not normally occur simultaneously throughout the system, except in some cases of order-disorder changes. Instead, due to thermal energy fluctuations of a statistical nature, a small number of atoms will overcome the energy barrier and enter the β-phase. Once this occurs the reaction proceeds by a process of growth. Change of phase by a nucleation and growth process requires considerably less energy than an instantaneous and homogeneous process.

Once some β-phase is nucleated there exists a possibility that the reverse reaction will occur. However, the net reaction will be towards the phase of lower energy. The rate of reaction is given by an Arrhenius relationship as expressed by the equations:-

$$R_{\alpha \rightarrow \beta} = A.\mathrm{Exp}[-(Q_1)/RT]. \quad - - - - \quad (1)$$

$$R_{\beta \rightarrow \alpha} = A'.\mathrm{Exp}[-(Q_2)/RT]. \quad - - - - \quad (2)$$

The pre-exponential factors A and A' can generally be taken to be equal, and it can be shown using transition state theory that

$$A \sim n.\frac{kT}{h}.\exp[\Delta F^*/RT],$$

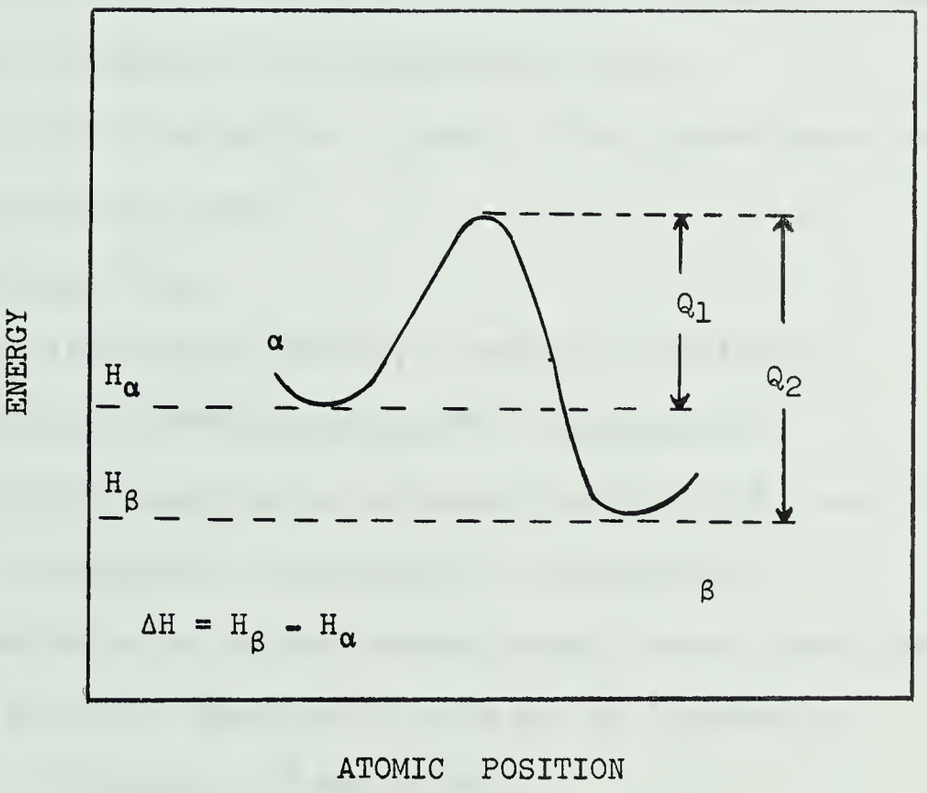

Figure 4. Energy Vs. Atomic Position Diagram.

where n is the number of single atom embryos, kT/h a universal frequency factor (h is planck's constant), and $\exp[\Delta F^*/RT]$ the probability that an embryo of critical size for nucleation will form, Thus,

$$R_{\alpha\rightarrow\beta} = \bar{A}\cdot\exp[-(Q_1 + \Delta F^*)/RT] \qquad - - - - \qquad (3)$$

and

$$R_{\beta\rightarrow\alpha} = \bar{A}\cdot\exp[-(Q_2 + \Delta F^*)/RT] \qquad - - - - \qquad (4)$$

where the pre-exponential factor $\bar{A}$ is assumed to be relatively independent of temperature compared to the exponential term.

The net rate of nucleation is equal to the forward minus the reverse reaction rates. Thus,

$$\begin{aligned}(R_{\alpha\rightarrow\beta})_{net} &= R_{\alpha\rightarrow\beta} - R_{\beta\rightarrow\alpha} \\ &= \bar{A}\cdot\{\exp[-(Q_1 + \Delta F^*)/RT] - \exp[-(Q_2 + \Delta F^*)/RT]\} \\ &= \bar{A}\cdot\exp[-\Delta F^*/RT]\cdot\{\exp[-Q_1/RT] - \exp[-Q_2/RT]\}\end{aligned}$$

Now the term in the braces can be replaced by $\exp[-Q'/RT]$, i.e.,

$$\{\exp[-Q_1/RT] - \exp[-Q_2/RT]\} \simeq \exp[-Q'/RT],$$

where Q' is some value for the activation energy barrier (see Figure 4) between Q_1 and $Q_1 + \Delta H$. Thus the net rate may be expressed as

$$(R_{\alpha\rightarrow\beta})_{net} = \bar{A}\cdot\exp[-\Delta G/RT], \qquad - - - - \qquad (5)$$

where $\Delta G = \Delta F^* + Q'$.

In practice the rate of nucleation is also influenced by energy terms of a non-thermodynamic nature.[10] Consider a reaction driven by a negative chemical energy change ΔG_c. When the nucleus forms the atoms at the interface occupy positions of compromise between the old and new structures, and as a result they have higher energies than the other atoms. This results in a positive surface energy term ΔG_s. When nucleation occurs in a solid the phase change is also accompanied by a

change in volume and shape. The resulting elastic strains imposed on the lattice produce a positive strain energy term ΔG_E. The reaction rate will now depend on the algebraic sum of all the energy terms, ΔG, where $\Delta G = \Delta G_c + \Delta G_s + \Delta G_E$. For nucleation to occur it is necessary that $|\Delta G_c| > |\Delta G_s + \Delta G_E|$, since ΔG must be negative.

The simple process of nucleation does not include an activation energy for diffusion. An overall transformation rate will, however, because the overall rate depends on grain or phase growth which may be diffusion controlled.

A phase change which occurs within a magnetic field gives rise to a magnetic energy term if the two phases have different susceptibilities. Taking the magnetic energy to be $1/2\chi H^2$, the change in magnetic energy, ΔG_M, due to the change from α to β phase is $1/2(\chi_\beta - \chi_\alpha)H^2$, where χ_β and χ_α are the susceptibilities of the two phases. Thus, the energy of nucleation, ΔG, is given by

$$\Delta G = \Delta G_c + \Delta G_s + \Delta G_E + \Delta G_M, \quad - - - - \quad (6)$$

or

$$\Delta G = \Delta G_{NM} + \Delta G_M, \quad - - - - \quad (7)$$

where ΔG_{NM} denotes non-magnetic energy terms. Thus the rates of nucleation outside and within a magnetic field are given by Equations (8) and (9) respectively.

$$\dot{n}_{NM} = B.Exp[-(\Delta G_{NM})/RT]. \quad - - - - \quad (8)$$

$$\dot{n}_M = B.Exp[-(\Delta G_{NM} + \Delta G_M)/RT]. \quad - - - - \quad (9)$$

The variation of the nucleation rate due to the presence of a magnetic field is dependent on the magnitude and sign of the susceptibility change.

III(a) GENERAL MAGNETIC EFFECTS

The effects of a magnetic field on chemical engineering systems has been extensively studied on a theoretical basis by Camp and Johnson. The study was undertaken with special reference to the problems of the stellarator, a device connected with controlled thermonuclear reactions. A component of the stellarator, the blanket, was required to operate under a magnetic field and to perform a three-fold function:

(i) act as a neutron shield.

(ii) extract thermal energy by absorbing kinetic energy from neutron reaction products.

(iii) provide a means of breeding tritium.

Although the main aim of the study was to evaluate the effect of a magnetic field on the performance of the blanket, the conclusions reached were deemed to be applicable to other systems.

The equilibrium thermodynamic properties in the presence of a magnetic field were studied in detail. Possible variations in chemical equilibrium and temperature of phase change were calculated from magnetic changes in thermodynamic quantities such as entropy, free energy and activity. The effect of a magnetic field on physical and chemical rate processes was discussed, mainly considering classical and irreversible thermodynamic laws. Fluid flow in a field was also studied, particularly the case of suspended particles.

On the basis of their observations Camp and Johnson concluded that for most para- and dia-magnetic systems at ordinary temperatures ($>50^{\circ}K$) magnetic effects were negligible; to obtain measurable magnetic effects "either extremely low temperatures, or extremely high magnetic fields, or both would be required".

Despite this pessimistic prediction, magnetic inhibition of diffusion has been observed for a non-ferromagnetic system.[3,4,11 & 12] A magnetic field has also been found to influence the grain growth of bismuth.[13]

(b) MAGNETIC INHIBITION OF DIFFUSION IN METALS

The effect of the electron drag on the electrodiffusion of metal ions has received extensive theoretical study.[14] After an exhaustive mathematical discussion, Ficks[15] concluded that the electron drag effect on the diffusion of metal ions "may be extremely large and may even determine the whole effect". This indicates that electrons do play an important part in determining the rate of electron diffusion of ions. Since the motion of an electron can also be considerably modified by the presence of a magnetic field,[16] this suggests that a field might affect the rate of chemical diffusion of ions.

An experiment showing the effect of a magnetic field on the diffusion rate of Cu atoms in Al-3%Cu solid solution has been discussed by Youdelis et al[4] and Colton.[3] Diffusion couples of alloy and pure aluminum were made by pressure welding at elevated temperatures. Each couple was halved; one section was allowed to diffuse inside a magnetic field and the other was treated similarly outside the field. This process annihilated the possibility of anomalous results occurring, arising from discrepancies in composition. The diffusivity values obtained for the no-field diffusion anneals were slightly higher than previously published results,[17,18] and this was attributed to the excellence of the welds obtained. Flat sandwich and cylindrical couples were used, the latter being designed to neutralise the possible effects of a Hall field. In fact, the dimensions of the weld area were such

that no Hall field was generated and both types of couples have similar diffusion results.

The diffusion rate in a magnetic field of 30 K. oersteds was found to decrease by a factor of 25% for a field perpendicular to the direction of diffusion. This result was found to be statistically significant to a 99% confidence level. A field parallel to the diffusion direction did not affect the diffusion rate.

For the field case the phenomenological laws of diffusion were obeyed, the Matano area being linearly proportional to the square root of time. Measurements of Kirkendall shifts obtained from penetration data showed no significant difference for field and no-field couples. This was taken to be an indication that the field inhibited the inter-diffusion process and not the intrinsic diffusion rates.

A theory based on the plasma-magnetohydrodynamic properties of the alloy was developed to account for the field diffusion inhibition. This theory, attributing diffusion inhibition to the action of electro-magnetic forces on the diffusion transported electrons, gave adequate quantitative agreement with experimental results. The constancy of the Kirkendall shifts obtained showed that the inhibition was due to a variation in the inter-diffusion rate and further supported the theory. In the theory the alloy was pictured as a two-fluid plasma. This could essentially be treated as a one-fluid plasma of electrons due to the electron mobility being substantially larger than that of the ions. Diffusion was deemed to be controlled mainly by the motion of the diffusion transported electrons. The tendency of the system to preserve electrical neutrality makes the ions follow the electrons, and thus by

influencing the motion of the electrons, a magnetic field also affected the motion of the ions. The situation described by Youdelis et al[4] is completely different from that considered by Ficks,[14,15] where an electric field imposed a net directed movement of electrons and ions with the resulting electron drag (due to bombardment) on the ions.

A solution of the equation of motion for an electron gas[16] shows that the electron diffusion current transverse to a magnetic field is dependent on the electron collision (ν_e) and cyclotron (ω_{ce}) frequencies; thus

$$j_\perp \propto \frac{1}{1 + \omega_{ce}^2/\nu_e^2} \qquad - - - - \qquad (10)$$

Due to the direct influence of the electrons on the ions in the attempt to maintain electrical neutrality, chemical diffusion is reduced in the same proportion. The diffusivity transverse to the magnetic field, $D_\perp$, is thus given by[4]

$$D_\perp = \frac{D}{1 + \omega_{ce}^2/\nu_e^2} , \qquad - - - - \qquad (11)$$

where D is the no-field diffusion constant.

The diffusion results obtained were not sufficiently accurate to indicate whether the field affected the frequency factor (D_o), the activation energy (ΔG), or both. A theoretical study of charge oscillation and charge screening showed that the effect of the field on the charge screening was not sufficiently large to affect diffusion via the activation energy. This conclusion was substantiated by the fact that for a field parallel to the diffusion direction no change in diffusivity was obtained. Thus any variation in the electron screening parameter

was considered too small to give rise to a noticeable activation energy change. Hence it was concluded that the inhibition in diffusion was due to a change in D_o arising from the plasma-magnetohydrodynamic influence of the field on the electrons.

(c) EFFECT OF A MAGNETIC FIELD ON TRANSFORMATION TEMPERATURE

Inhibition of diffusion due to the presence of a magnetic field was also found to take place in liquid metals. Youdelis et al[12] and Cahoon[11] studied the effects of a field on the solidification process of alloys. Solidification segregation in Al(rich)-Cu alloys was found to increase by about 30% and 50% for fields of 13 and 34 K. oersteds respectively, the effect being independent of field direction. For the Bi(rich)-Sb system segregation decreased by 60% in a 13 K. oersteds field. These changes in solidification segregation were adequately explained in terms of the standard solidification equations,[19,20] subject to a magnetic inhibition of diffusion. Considering the metal as a plasma and applying irreversible thermodynamics, Youdelis et al[12] developed a theory which explained the results. Diffusion inhibition caused a non-equilibrium concentration change at the solid-liquid interface, and this effectively raised the liquidus temperature of the alloy (Figure 5). This theory was found to be consistent with heat flow requirements for a system solidifying under conditions of a diffusion "constraint". The shift of the liquidus line could not be explained as a direct effect of the magnetic energy term on the solidification temperature or phase diagram. The component of magnetic energy change during solidification, arising from the difference in susceptibility of the liquid and solid metals, was found to be negligibly small compared

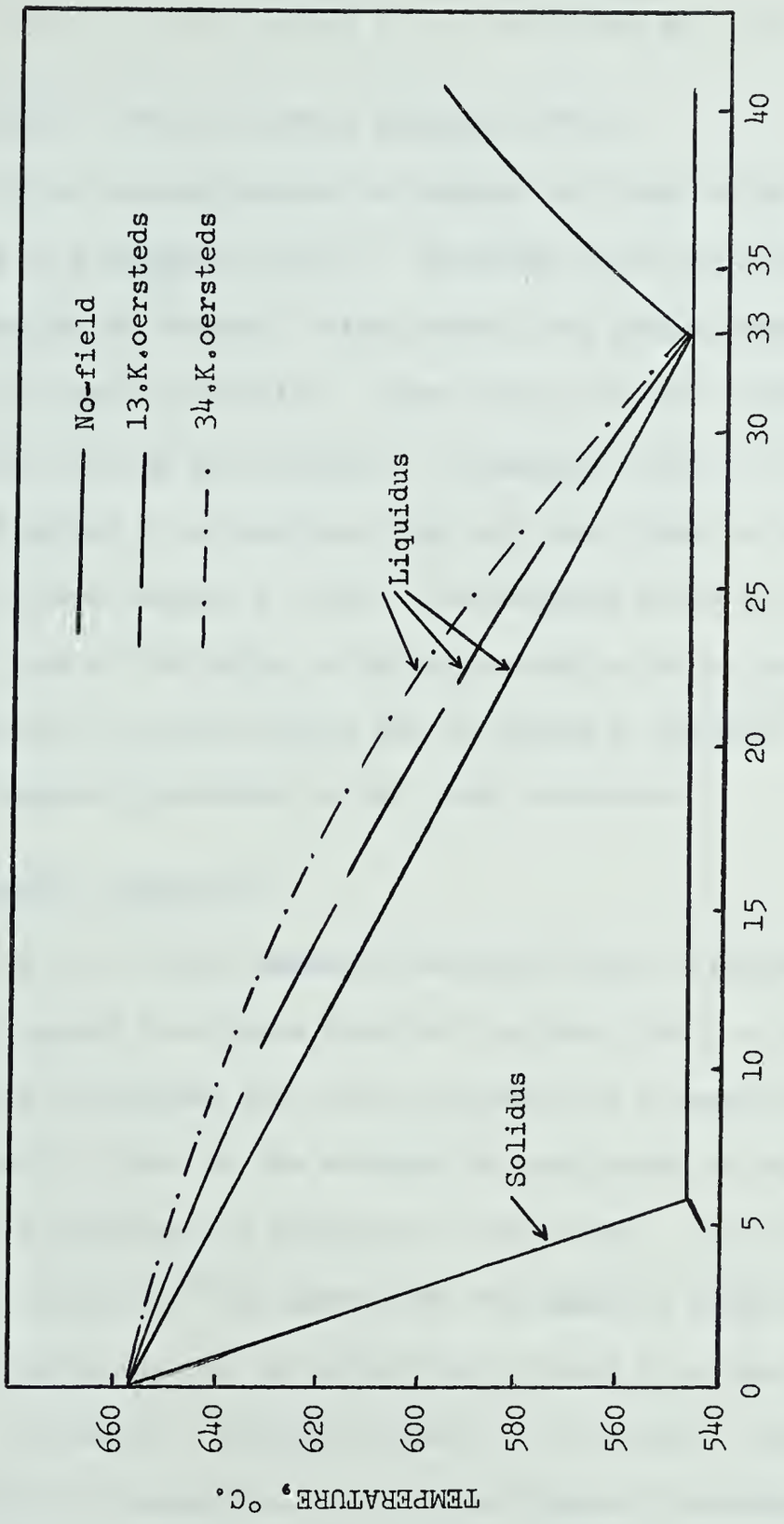

Figure 5. Magnetically induced shifts in Liquidus line of the Constitution Diagram of Al-Cu alloy.

to the heat of solidification of 11.8 calories per gram.

(d) MAGNETIC EFFECT ON GRAIN BOUNDARY MOTION

Grain boundary motion in bismuth was found to be affected by the presence of a magnetic field.[13] Although Bi is only slightly dia-magnetic, free energies of magnetic origin within the grains generate forces which act on the grain boundaries. These forces produce markedly preferred orientation during grain growth in a magnetic field. The fully grown grains obtained in a magnetic field are also found to be smaller than those obtained without a field. The magnetic field also causes an unusual kind of 'sticking' of grain boundaries which normally exhibit high mobility. These results are explained by Mullins[13] as the effects of the magnetic pressures on the grain boundaries.

(e) MAGNETIC ANNEALING

Due to the high magnetic susceptibility of ferromagnetic metals it would appear that these would be the most likely to exhibit changes in physical processes due to the influence of a magnetic field. Unfortunately, most of the evidence at hand seems to suggest that only magnetic properties are affected to any extent. Considerable work on magnetic annealing[22] has shown that the magnetic properties of ferro-magnetic materials may be extensively altered by annealing in a magnetic field. The magnetic energies induced by the field, though often substantial by comparison with no-field magnetic energies, tend to be insignificant when compared with the energies required for precipitation, recrystallization and other physico-chemical processes.

The effect of magnetic annealing is to exaggerate any anisotropies

existing in the material along the field direction; both magnetic and physical properties may be affected. Kaya[23] suggests that needles of ordered material formed within the metal matrix would line up parallel to the field during magnetic annealing whilst de Jong et al[24] have shown conclusive evidence that the grains of Ticonal X (an alloy similar to Alnico-5) are substantially elongated in the field direction after magnetic annealing.

Published reports have claimed that magnetic annealing may influence the mechanical properties of steel.[25] This appears a plausible proposition, particularly since it is recognised that the morphology of a material may be influenced by magnetic annealing. However, these reports concerning the effect of a field on mechanical properties have not been thoroughly accepted or confirmed.

EXPERIMENTAL

I. THE MAGNET

The field used for the ageing experiments was provided by a water cooled, pole type electromagnet which is an adaptation of the Upsalla magnet.[26] (Details of the construction are given by Colton).[3] With the pole pieces at 1 1/2" separation the magnet could provide a maximum field of 35 K. oersteds, but was regulated to 30 K. oersteds for continuous operation. The field generated was uniform to ±3% over a cylindrical volume 3 1/2" in diameter by 1 1/2" in length. The magnet was water cooled to permit prolonged operation at high power levels without excessive heating. Power was supplied by a 36 kilowatt, d.c. constant voltage (ripple 2%) generator.

II. PREPARATION OF SPECIMENS

Three types of Al(rich)-Cu alloys were investigated:

(a) alloy cast from 99.999% pure Al and 99.9999% pure Cu. Composition about 3.5% Cu.

(b) alloy cast from 99.9% pure Al and 99.9% pure Cu. Composition from 4.0 to 4.9% Cu.

(c) factory made commercial alloy containing about 4.7% Cu and about 0.8% Si.

The aluminum and copper metals were prepared for casting by cleaning small blocks of the metals in hydrochloric and nitric acid respectively. The alloy was made up in batches of 150 to 250 grams with a statuary weight composition of about 4.5% Cu. The aluminum, contained in a graphite crucible, was first melted in an electric muffle furnace at about 1350°F. A measured amount of copper was then added to

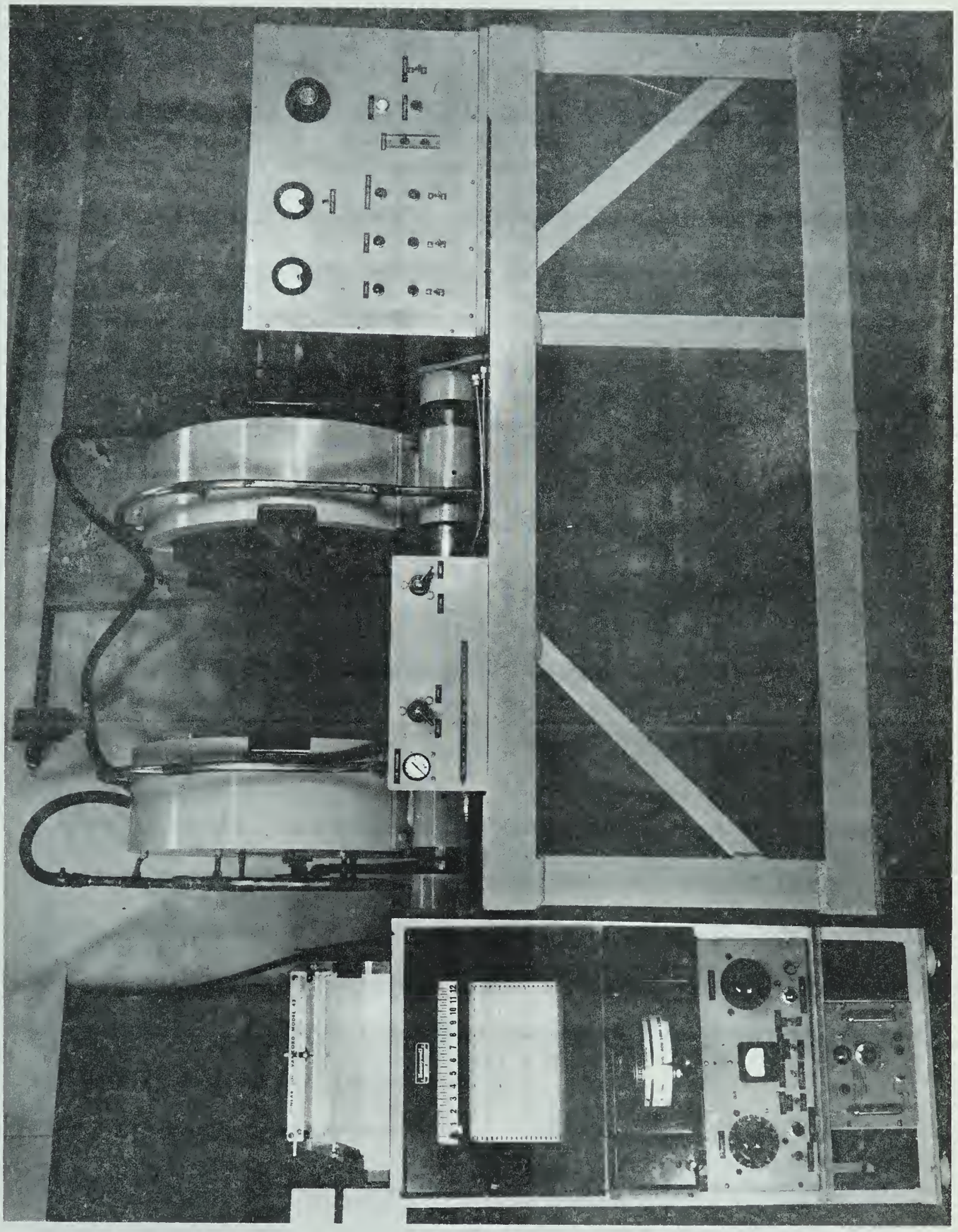

Figure 6 - Photograph of Electromagnet.

the molten aluminum. The melt was thoroughly mixed by pouring back and forth between two crucibles about eight times, degassed by bubbling with argon and skimmed to remove the oxide layer which formed at the surface. The melt was then poured into open ended graphite moulds which were mounted on steel plates, the plates being cooled with water jets to insure unidirectional solidification. Cylindrical ingots about 11 cms. by 1.9 cms. were obtained. To minimize variations in composition due to segregation during solidification the ingots were cropped (about 1 cm. from the chill face and 2 cms. from the hot end), the central section being considered essentially homogeneous in composition.[11,12,19,20]

The cropped ingots were then cold worked and swaged to a diameter of 1.4 cms. in order to close up any porosity arising from gas evolution during solidification. The ingots were machined on a lathe to produce uniform cylinders free from surface contamination.

The alloy was homogenized for seven days at 540°±10°C, quenched and cut into small cylindrical specimens about 1.4 cms. in diameter and 0.4 cm. in height. The commercially made alloy was not cold worked but was homogenized and cut to the same dimensions as the cast alloy.

The flat surfaces of all specimens were ground down on increasingly fine emery paper and finished on grit 500 emery paper. The composition of the specimens in their final form was checked and evaluated by X-ray analysis in a Phillips Flourescence unit.

Discrepant results due to room temperature ageing were avoided by solution heat treating specimens immediately prior to ageing treatments. Solution heat treatments were carried out in an electric tube furnace coupled to a high-low temperature control unit. The specimens

were kept at 550°±3°C for 90 minutes. This temperature was carefully reproduced for different treatments* to prevent variations in vacancy concentration; the vacancy concentration can influence the ageing rates of some alloys. After heat treatment the specimens were quenched in cold water.

Some of the specimens were cold worked in the solution heat treated condition, prior to ageing. The cylindrical specimens were rolled, this process being accompanied by an increase in the diameter of the specimens along the direction of rolling and a decrease in the height of the specimens. The reduction in height of the specimens was used as a measure of the amount of cold work they had received. Specimens cold worked 10% (height reduction) were passed through the rollers about ten times, the separation of the rollers being reduced very slowly to avoid excessively straining the specimens which might have caused some cracks. Two or three passes through the rollers were sufficient to obtain 2.5% cold work.

III. AGEING ANNEALS

Specimens of Al-Cu alloy were aged in and out of a magnetic field to investigate the effect of a field on the ageing rate. The degree of ageing was determined by hardness measurements. An ageing temperature of 190°C was generally used, it being indicated by previous data that this temperature gave a large variation in hardness (about 40 D.P.H. units) combined with short ageing time.[9]

---

*A number of specimens were heat treated together, care being taken to include in the same batch specimens or semi-specimens to be aged for corresponding times in and out of the field.

Hardness curves were established using single and multiple specimens in four methods:

A.M.*(1) A series of specimens were aged for different times in the field. Another series of specimens were treated outside the field. Each specimen yielded one hardness value only. Care was taken to select specimens of near identical composition for field and no-field anneals of equal periods of time.

A.M. (2) About seven or eight specimens were halved. Corresponding halves were aged in and out of the field for equal periods of time.

A.M. (3) In this method a single specimen was used. During ageing the specimen was periodically removed from the furnace, quenched, polished, tested for hardness and returned to the furnace. After the no-field run the specimen was re-solution heat-treated and aged in the field in the same manner. The ageing time was taken as the total time the specimen spent in the furnace. The length of time specimens spent outside the furnace was about the same for field and no-field runs.

A.M. (4) A single specimen was halved; each half was aged in and out of the field by the method of periodically interrupted anneals as described in A.M. (3).

---

*A.M. indicates 'ageing method'.

All four methods gave similar ageing curves. A.M. (1) suffered from larger hardness errors than the others and A.M. (3) was viewed with suspicion due to the possibility of extraneous results arising from the cycling procedure. The remaining two methods seemed to be equally sound and A.M. (4) was adopted for most of the experiments due to its inherent economy of time and material.

The samples were aged in the centre of a tube furnace and were supported in either of two ways:

(a) A single specimen was wrapped in aluminum foil with a measuring thermocouple embedded into it. (Figure 7(a)).

(b) One or more specimens were placed in a closed Al-Cu alloy boat. The temperature was measured with a thermocouple embedded in a thick Al-Cu block placed inside the boat. Up to four specimens could be accomodated in this way and annealed simultaneously. (Figure 7(b)).

Both types of support were considered to protect the specimen efficiently and to give accurate readings of the specimen temperature. The measuring thermocouple was inserted into a well drilled into the metal and contact between the thermocouple junction and the metal was prevented by a small silica ring placed at the bottom of the well. (Figure 8).

Ageing was carried out under an argon atmosphere at a pressure of about 5 cms. of mercury. The furnace was purged with flowing argon prior to an anneal and every 12 hours during the anneal. Little oxidation of the specimens, foil or boat was observed.

The furnace consisted of a thin-walled silica tube, eighteen inches long with Kanthal A ribbon heating element would uniformly around the central nine inches of its length. The heating element was

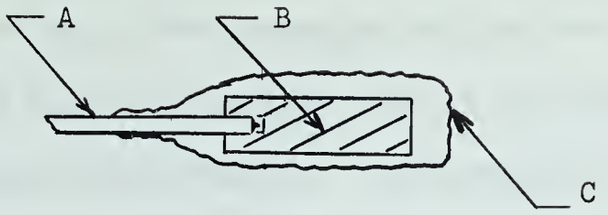

Figure 7(a). Foil wrapped specimen. A, thermocouple. B, specimen. C, aluminum foil.

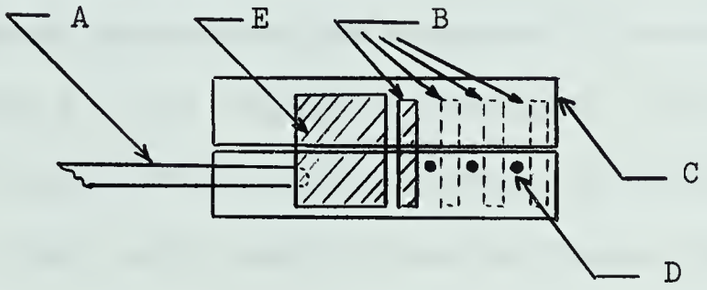

Figure 7(b). Specimen in Al-Cu alloy boat. A, thermocouple. B, specimen. C, hollow Al-Cu alloy boat. D, chromium wires to separate specimens. E, Al-Cu alloy block.

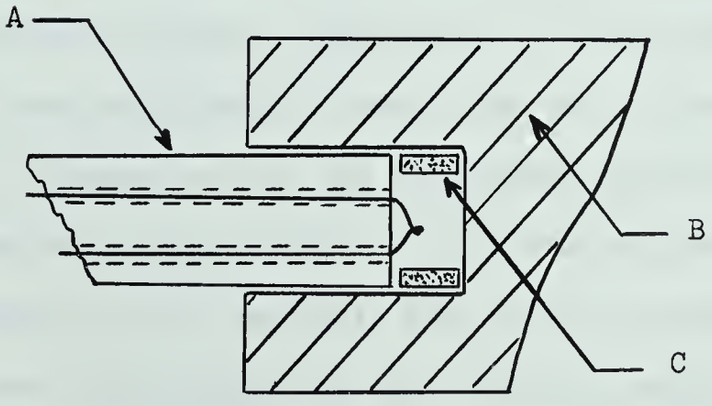

Figure 8. Thermocouple in specimen well. A, thermocouple. B, specimen. C, silica separating ring.

insulated with asbestos tape and asbestos cement. Figure 9 gives details of the end caps, thermocouples and the rest of the assembly. Porous plugs were placed at extreme ends of the central section in order to reduce the temperature gradient. The temperature gradient along the central section of the furnace was measured (see Appendix V, Figure 39). A temperature variation of about 1°C was found to exist within the central two inches, where the sample was located. Identical furnaces were used for field and no-field runs.

The furnace temperature was regulated by an automatic temperature controller working on the 'high-low' principle. The controller was sensitive to a signal from a control thermocouple and switched a relay to 'low' and 'high' power supplies when the furnace temperature became higher and lower (respectively) than the desired set temperature. The relay worked through two transformers so that 'high' was adjusted at a power setting giving a maximum temperature a few degrees above the ageing temperature; 'low' was adjusted to give a maximum temperature a few degrees below the ageing temperature. Two different controllers were used: a Wheelco Capacitrol Model 252P and a Thermo Electronic Model 80025. In about half of the experiments carried out, the Wheelco controller was used with the field furnace and the Thermo Electronic controller was used with the no-field furnace. The controllers were interchanged for the remaining experiments.

Both controllers were extremely sensitive, permitting excellent temperature reproduceability and controlling the specimen temperature to within $\pm$0.5°C. The furnace located in the magnetic field was suppled with d.c. power since a.c. power would cause vibrations and disrupt the bindings.

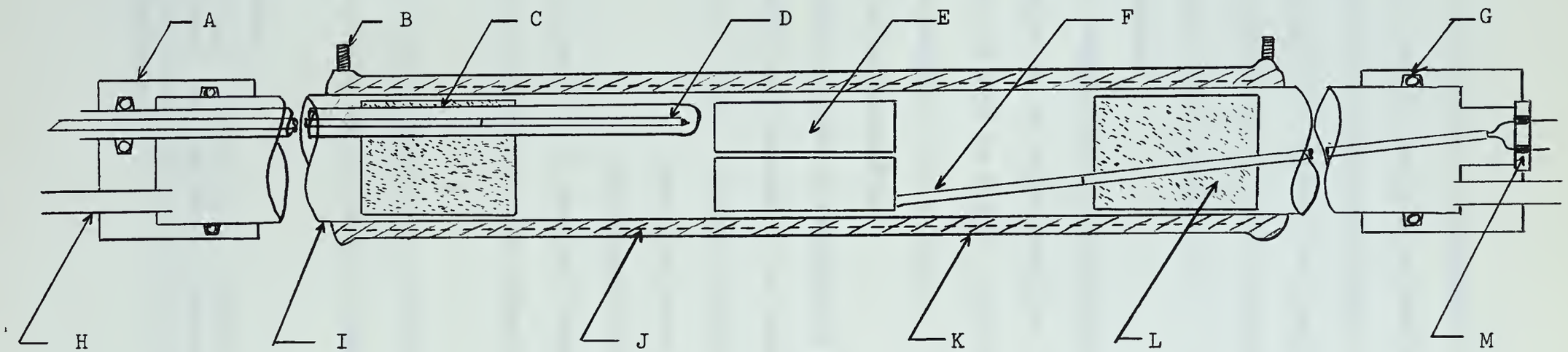

Figure 9. Furnace used for the diffusion anneals. A, brass end piece; B, terminal; C, control thermocouple shield (silica tube), D, control thermocouple; E, sample contained in alloy boat; F, measuring thermocouple; G, 'o'-ring seal on end piece; H, gas inlet tube; I, silica furnace tube; J, Kanthal A winding; K, insulation; L, porous plug; M, Stupakoff insulator.

Control and measuring thermocouples for both furnaces were of Cromel-P-Alumel wires and were made from the same spools. The measuring thermocouples were calibrated against a standardized Platinum-Rhodium thermocouple to investigate possible discrepancies in e.m.f. arising from inhomogenieties in the composition of the wires. At 190°C both thermocouples gave identical e.m.f. readings, about 1.5°C below the true temperature.*

Specimen temperatures were measured on a Honeywell Potentiometer Model 2745 through an ice point junction. Measurements could be made to an accuracy of 0.05°C at 190°C. The temperature setting of the controllers was adjusted with reference to the specimen temperature as registered by the potentiometer.

Between spot checks on temperature a continuous record of the sample temperature was obtained on an automatic recorder. The following recorders were used: Photovolt Varicord Model 43,

Westronics Model m11 b/u.dv24,

and Honeywell Model Y153X(67)-P6H.

Thus large discrepancies in specimen temperatures arising from possible faults in the controllers could be detected and the specimens involved discarded.

A continuous record of the current passing through the magnet was also kept; the fluctuation was of the order of 2.5%.

---

*Colton[3] used thermocouple wires from the same spools used in the present experiment. He calibrated them against NRC standards and the melting points of Al and An but did not report any variations in e.m.f. due to inhomogenieties.

IV. HARDNESS MEASUREMENTS

Specimens were prepared for hardness measurements by chemical polishing. The acid mixture* used was

80% concentrated phosporic acid,

12% concentrated sulphuric acid,

8% concentrated nitric acid.

The specimens were individually submerged in the acid for three minutes at 90°C with the surface to be tested facing down. A pair of tongs with dummy ends made of Al-4%Cu alloy was used to support the specimens, thus avoiding any cathodic reaction between the specimen and the tong material. The specimens usually emerged from the polishing mixture covered by a thin brownish film, but this was readily removed by rubbing lightly with a wet optical paper tissue, leaving a bright, even, high quality finish.

Mechanical polishing was avoided due to the possibility of work hardening the alloy and was only used for specimens which were to be studied metallographically. However, no perceptible variation in hardness values was observed between specimens polished chemically and mechanically.

Semi-micro hardness measurements were obtained using a Tukon Tester, with a diamond pyramid indenting point and a 1000 grams load. Micro-hardness measurements would not have been truly representative since indentations could be made wholly on a precipitate particle or on the matrix and discrepant results would be obtained. The small size of

*This mixture was used successfully by Colton[3] on Al-3%Cu alloys.

the specimens used made the use of a Rockwell macro-hardness tester impractical.

Each hardness value obtained was a mean measured from a total of 10 or 15 indentations placed along 2 or 3 traverses across the central section of the specimen (see Figure 10). Both diagonals were measured in each indentation, and in case where the diagonals differed by more than 25 filar units the reading was disregarded and a new impression made. Also neglected were indentations which appeared to be badly mishapen due to inclusions, grain boundaries etc.

V. METALLOGRAPHY

Samples designed for metallographic study were mechanically polished on a series of laps, the final polish being obtained on a slow moving Buehler Microcloth (AB) with 0.05 micron alumina abrasive. The laps were kept well lubricated with soap to prevent abrasive particles from becoming embedded in the sample. High quality polishes were obtained but the etched metal showed dark, uneven spots which were interpreted as impurities. These spots were found in approximately equal quantities at all stages of ageing and in the 'as cast' material; it was concluded that they were due to impurities inherent in the material and not abrasive particles or polishing pits.

The specimens were etched in Keller's Etch* for about 10 or 15 seconds. After etching the specimens were thoroughly rinsed in water, wetted with alcohol, and dried in a warm stream of air.

Photomicrographs at magnifications of 200X and 1300X were taken

---

*Keller's Etch contains 1/2% hydroflouric, 1 1/2% hydrochloric; and 2 1/2% nitric acids, and 95 1/2% water.

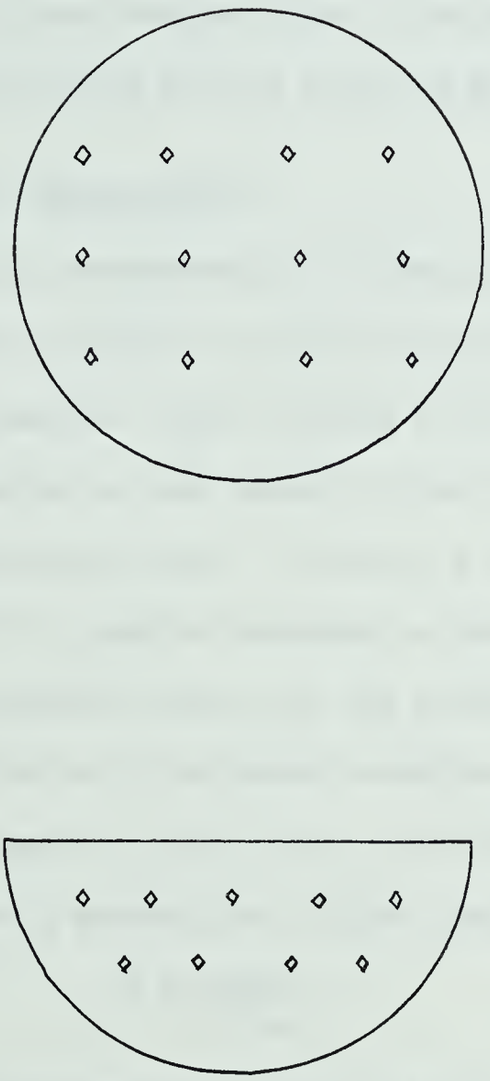

Figure 10. Typical distribution of hardness indentations along traverses on the specimens.

in order that structures for field and no-field specimens could be compared at corresponding ageing times. Structures were observed in the solid solution state, at the point where 95% of maximum hardness was reached, and in the overaged state. The photomicrographs were obtained on polaroid films using a Reichert MeF reflecting microscope.

VI. SUSCEPTIBILITY MEASUREMENTS

Susceptibility measurements were obtained using the Gouy method.[27,28] This experiment consists essentially of suspending a thin cylindrical specimen from a balance in such a way that it is partly inside a region of high magnetic field (see Figure 11). The magnetic forces generated tend to attract a para-magnetic specimen into the field and to repel a dia-magnetic specimen out of the field. By balancing the specimen first with the electromagnet current switched off and then with the magnet energized, the strength and direction of the magnetic forces can be evaluated.

The force on a particle in a field gradient is given by

$$f = kvH\frac{\partial H}{\partial s}, \qquad - - - - \qquad (12)$$

where k is the volume susceptibility, H is the magnetic field strength, s is distance and v is the volume.

If one end of the sample is kept in a region of high field and the other is in a region of zero field, the force on the whole sample may be obtained by integrating Equation (12) from maximum field to zero field along the axis of the specimen. The total force on the sample is

$$F = 1/2kH^2A \qquad - - - - \qquad (13)$$

where A is the cross sectional area.

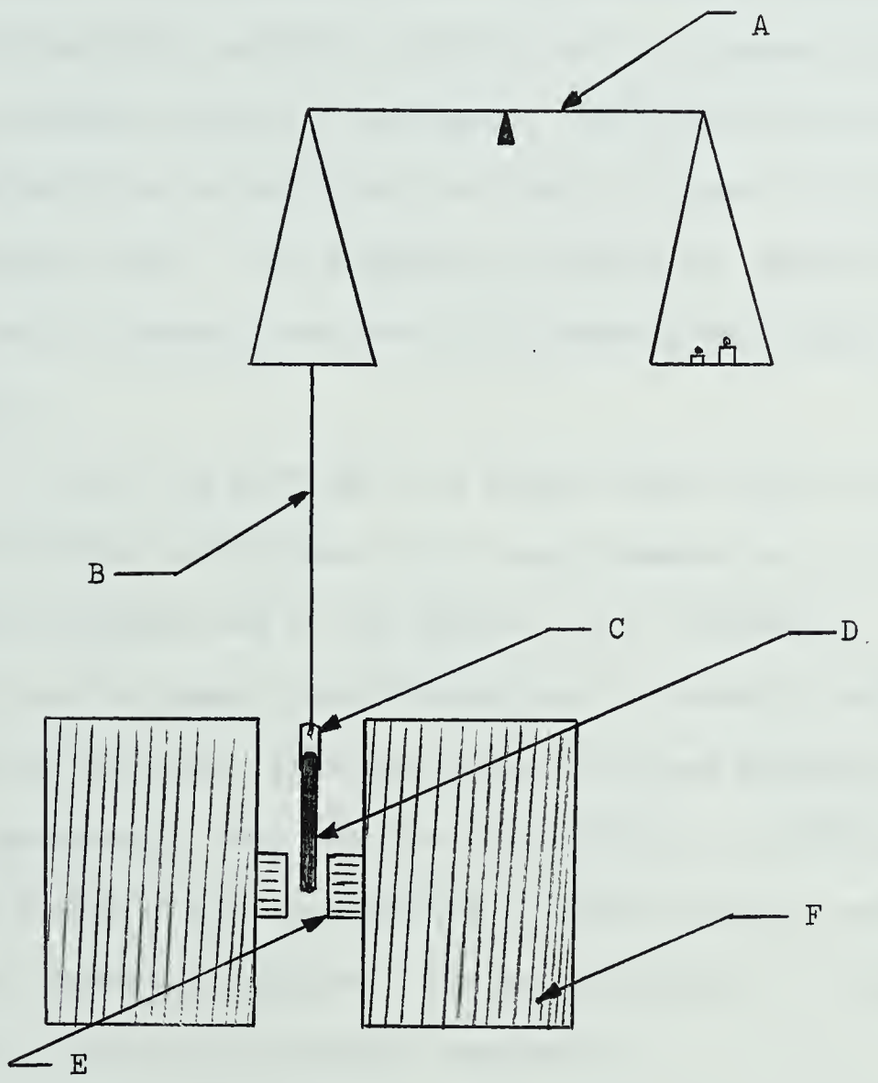

Figure 11. Gouy balance and magnet diagram. A, balance. B, suspension chain. C, nylon clasp. D, specimen. E, pole pieces. F, electromagnet windings.

In the present investigation cylindrical specimens 0.25 cms. in diameter and 2.5 cms. long were used. The samples were held in a small nylon clasp and suspended by a thin copper chain from one of the pans of a precise Becker balance capable of measurements with an accuracy of $\pm$0.1 m.g. The suspension system was designed so that the specimens hung vertically and centrally between the pole pieces with their lower ends in the exact centre of the poles. The length of the specimens was considered to be sufficient for their top ends to be in a region of negligible field. The suspension, balance and magnet were protected from stray air currents and the whole assembly was placed in a vibration free room.

The field was provided by a Neuport Pagnet Type O electromagnet with cylindrical pole pieces of 3.7 cms. diameter set 1.0 cm. apart. The field developed was in the region of 7 K. oersteds.

Since the exact field strength was not known, a calibration was carried out using pure aluminum, copper and lead specimens. Susceptibility measurements were made for Al-4.5%Cu and Al-4.7%Cu-0.8%Si alloys at three stages of precipitation, i.e. solid solution, maximum hardness, and overaged conditions. The susceptibility of θ-phase composition Al-Cu alloy was also measured.

A series of consecutive measurements were carried out for each sample. To avoid errors due to residual magnetism measurements were taken about 4 minutes after de-energizing the magnet, a preliminary study having shown that after three minutes the residual magnetism became negligible.

RESULTS

I. AGEING

The results of the ageing experiments are presented in graphical form, shown in Figures 12 to 26 inclusive. The caption to the Figures give the nominal composition, ageing temperature, and mechanical condition of the alloy. Since experimental conditions varied slightly in the different ageing experiments, the precise composition, ageing temperature, method and polishing procedure related to each Figure is given in Appendix I. An activation energy plot, obtained from results of the present experiment and the results of Silcock et al[9] is shown in Figure 27.

II. SUSCEPTIBILITY RESULTS

Information related to susceptibility measurements is presented in Table I. Known volume susceptibilities of the standards (Al,Cu & Pb) are plotted against the magnetic force Δw (see Appendix VI, Figure 40). The susceptibilities of the alloys were obtained by comparing measured magnetic forces against the calibration curve.

III. METALLOGRAPHIC RESULTS

A series of metallographs taken at magnifications of X200 and X1300 (Figures 28 to 37) illustrate the variation in the structure of the alloy as ageing progresses.

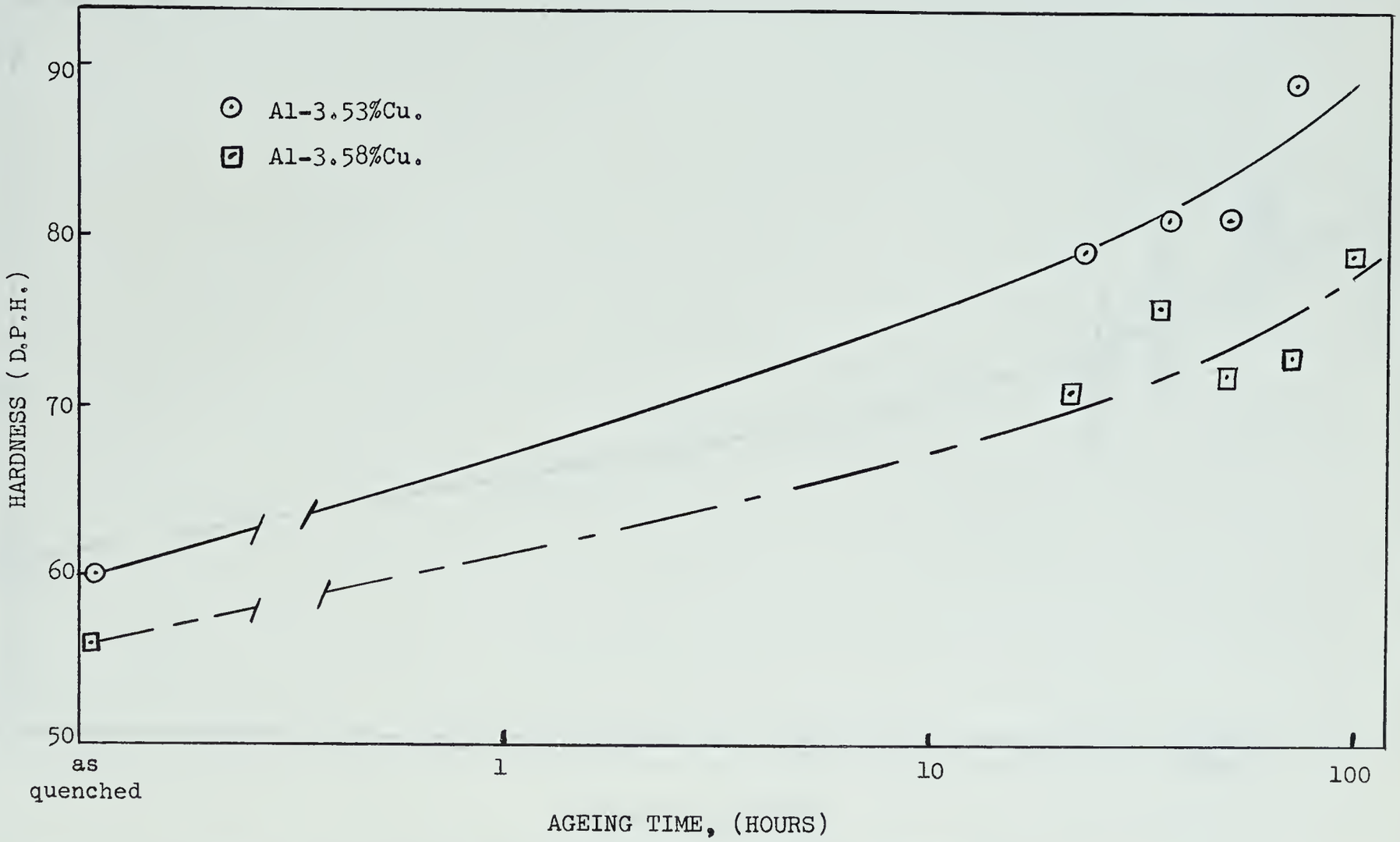

Figure 12. Unworked Al-Cu alloys aged at 22°C. (Appendix I, A and B).

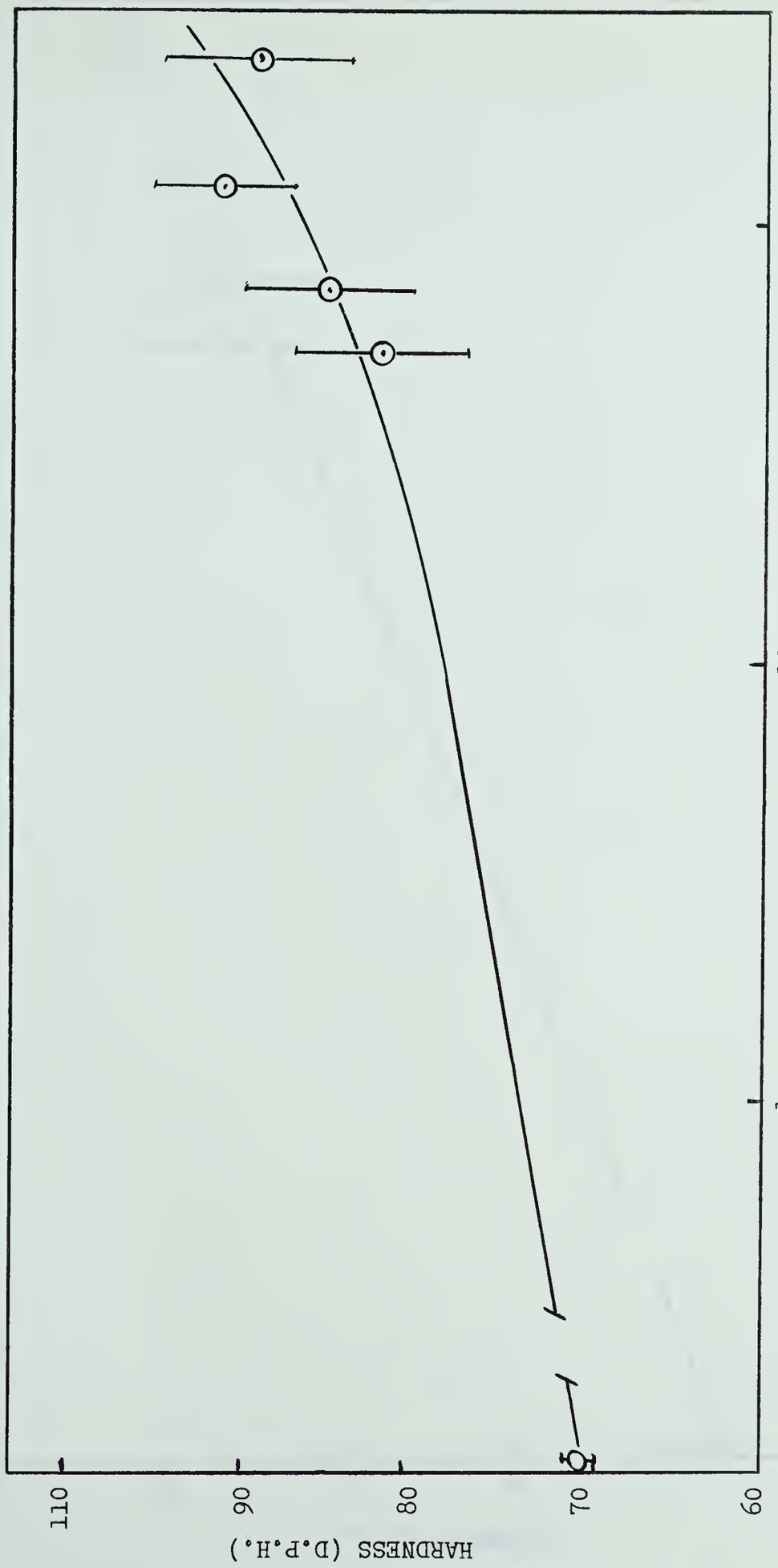

Figure 13. Unworked Al-4.7%Cu-0.8%Si alloy aged at 22°C. (Appendix I, C.)

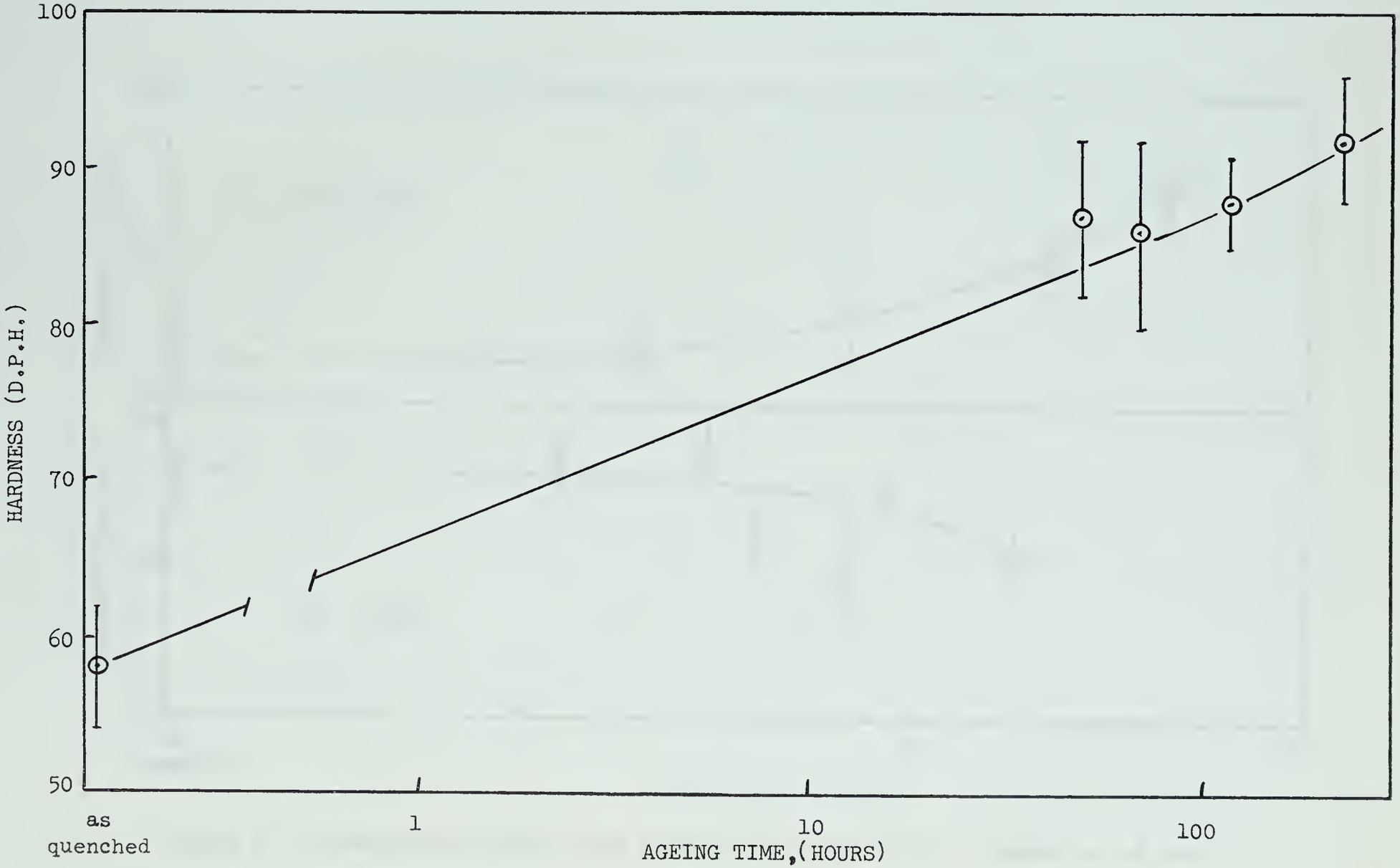

Figure 14. Unworked Al-4.1%Cu alloy aged at 22°C. (Appendix I,D.)

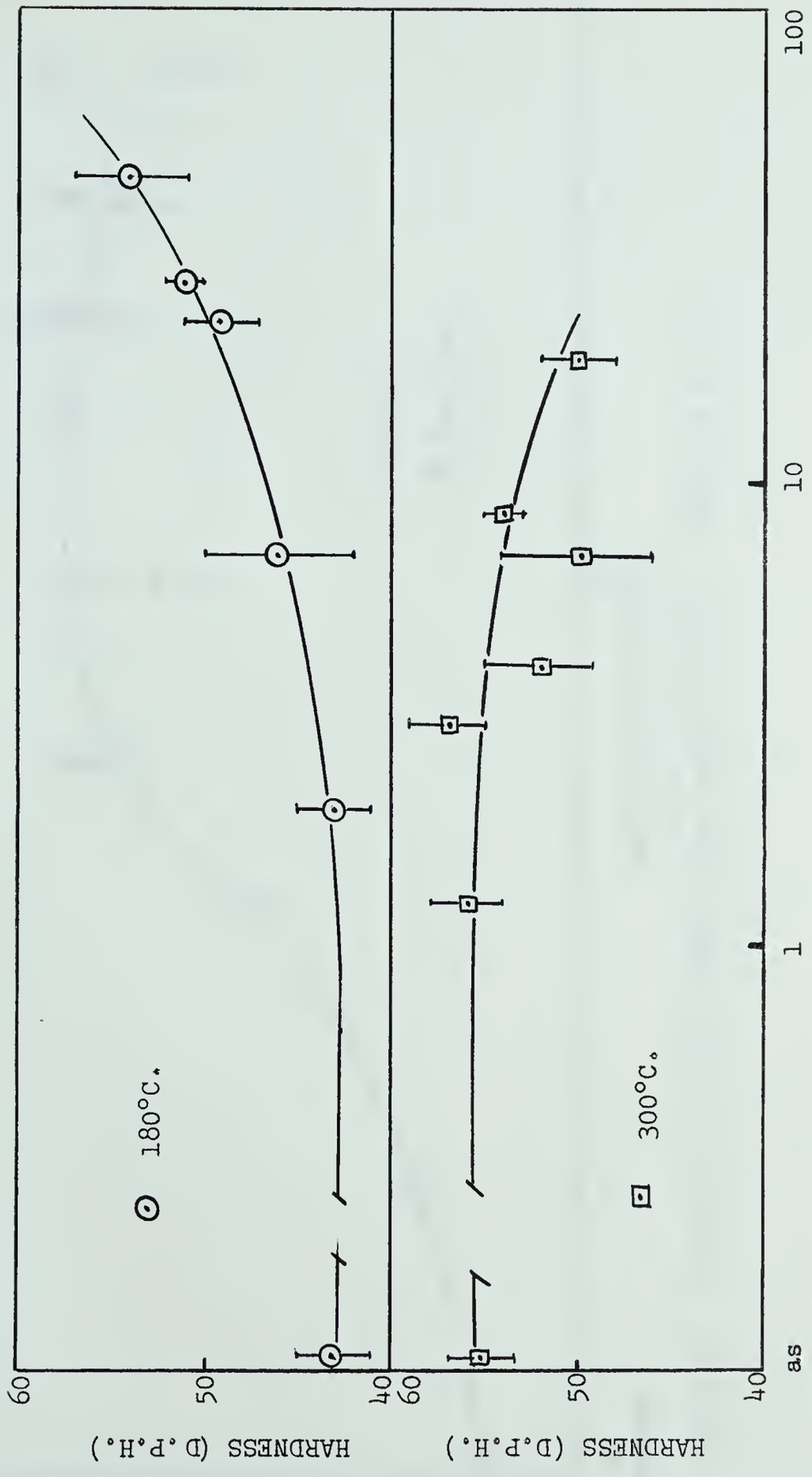

Figure 15. Unworked Al-3.6%Cu alloy aged at 180°C and 300°C. (Appendix I, E and F.)

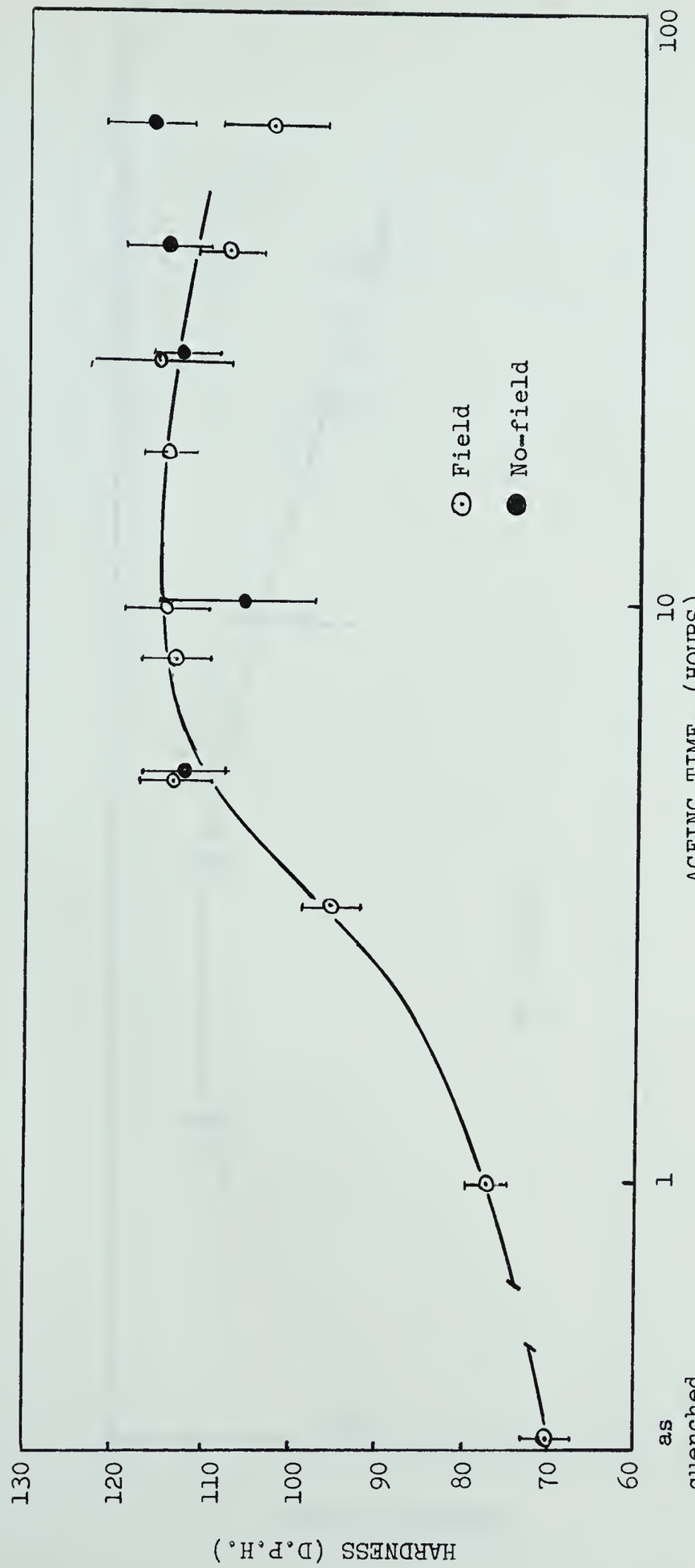

Figure 16. Unworked Al-4.7%Cu-0.8%Si alloy aged at 180°C. (Appendix I, G.)

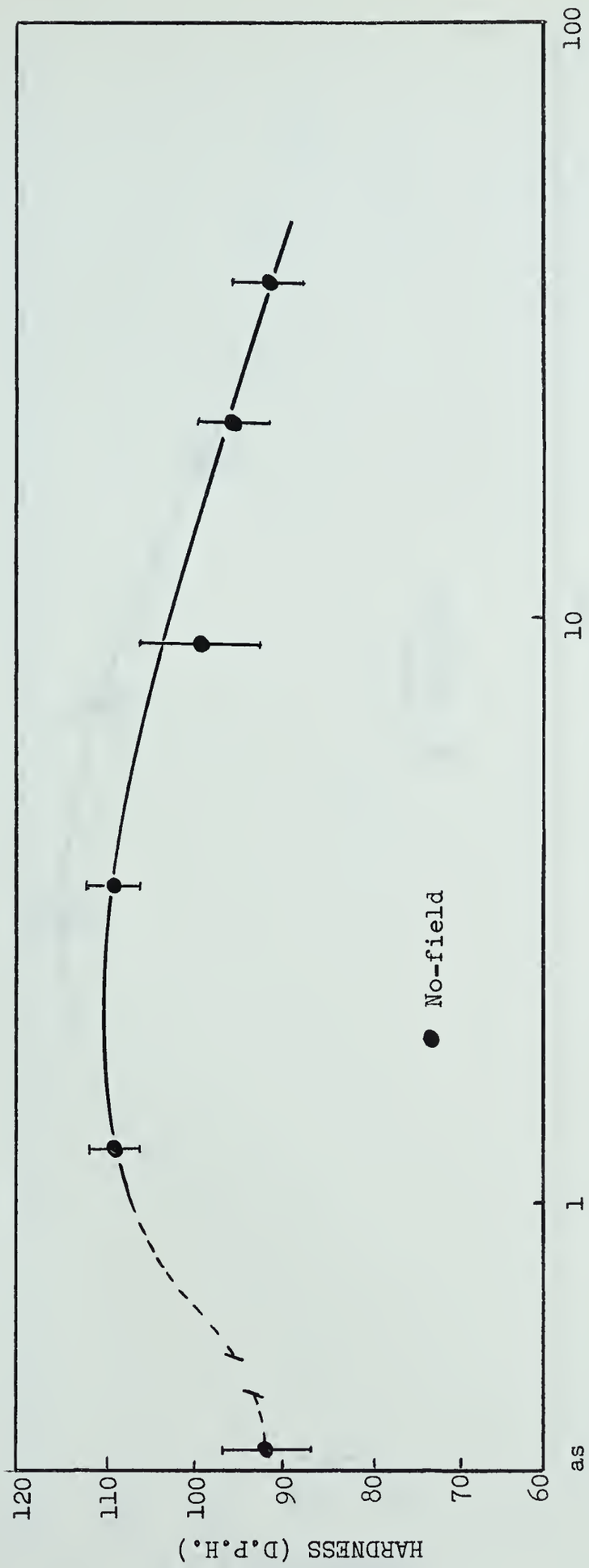

Figure 17. 10% cold worked Al-4.63%Cu alloy aged at 190°C. (Appendix I, J.)

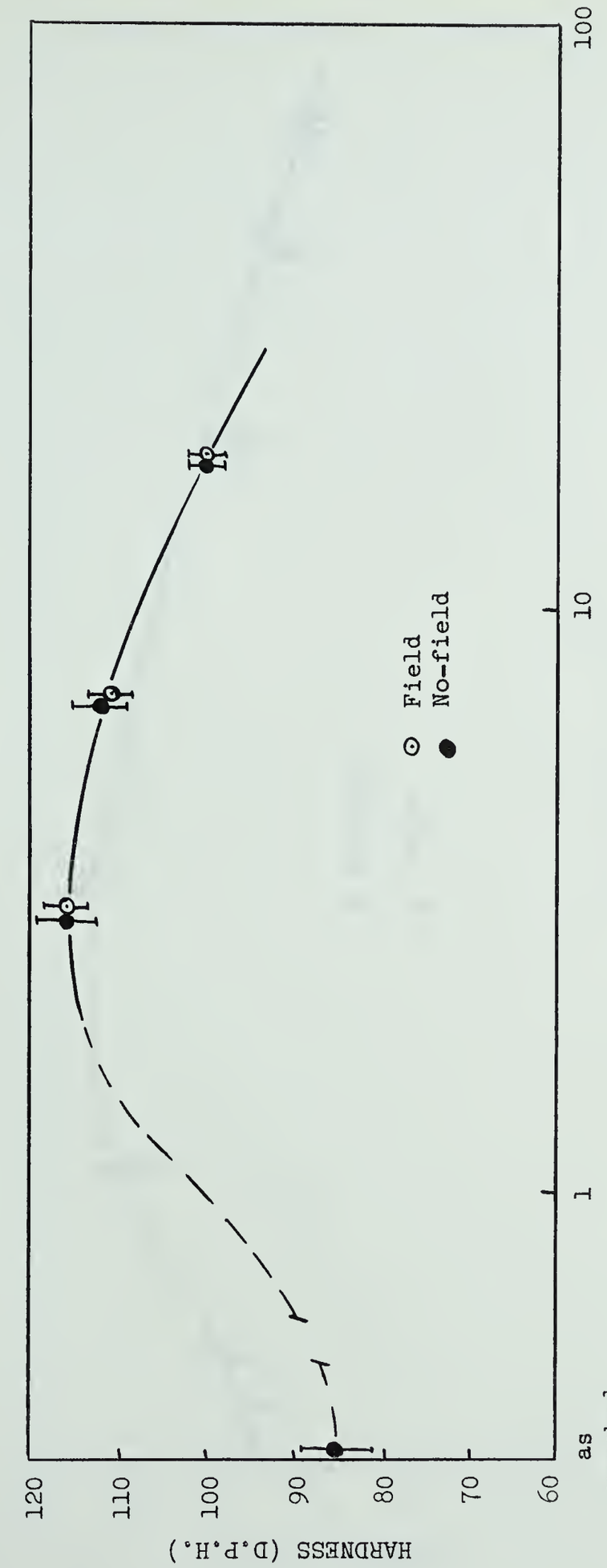

Figure 18. 10% cold worked Al-4.96%Cu alloy aged at 190°C. (Appendix I, K.)

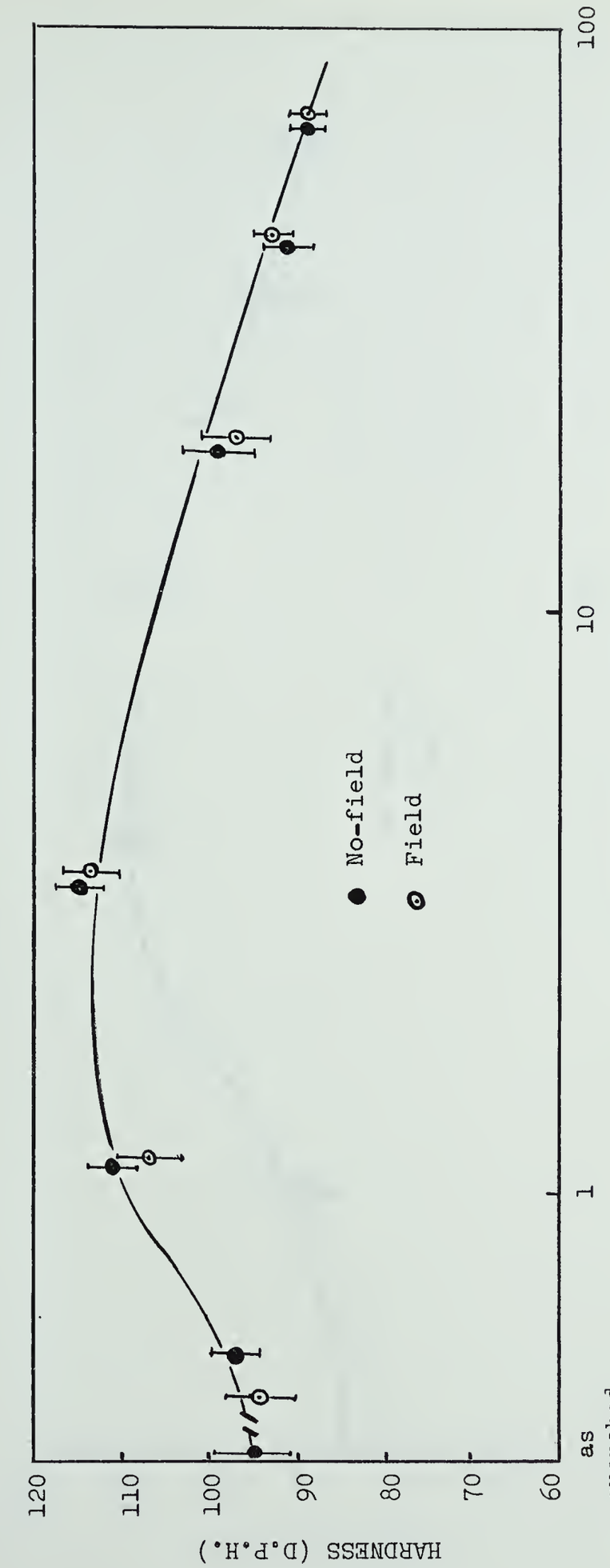

Figure 19. 10% cold worked Al-4.77%Cu alloy aged at 190°C. (Appendix I, L.)

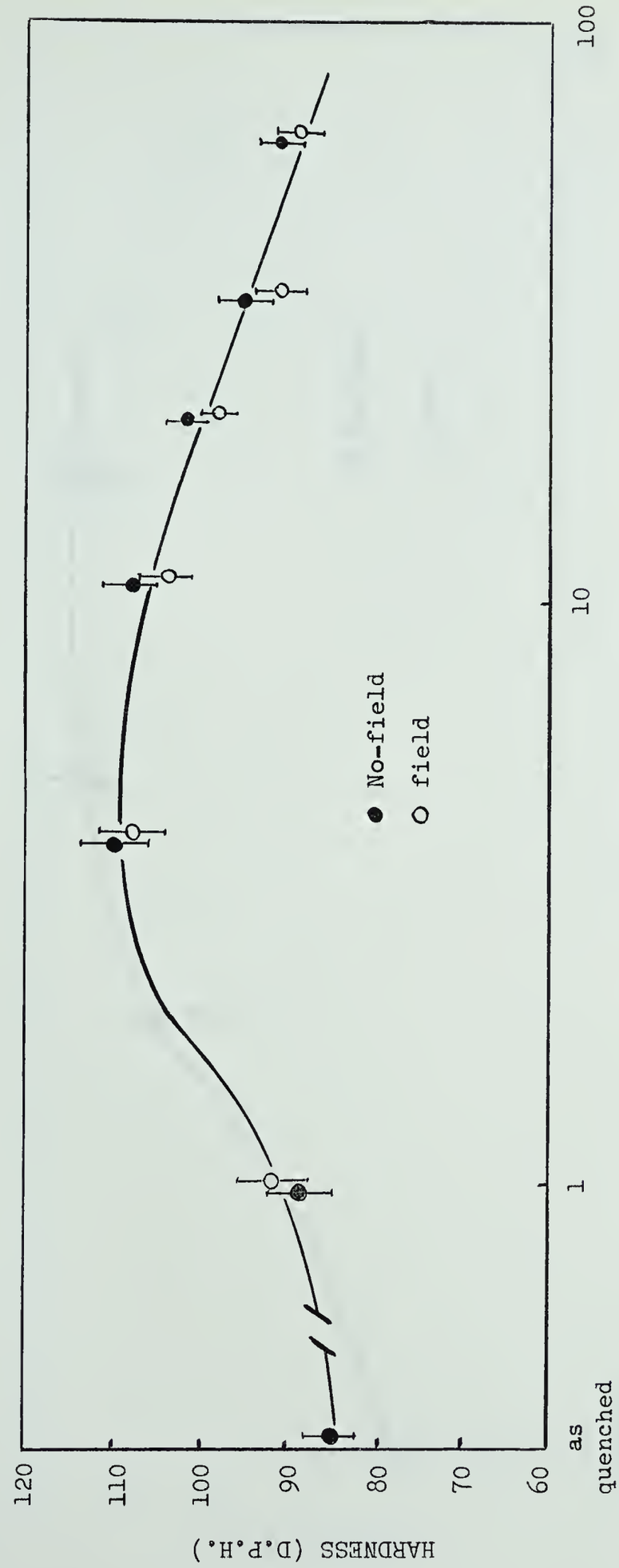

Figure 20. 2.5% cold worked Al-4.68%Cu alloy aged at 190°C. (Appendix I, M.)

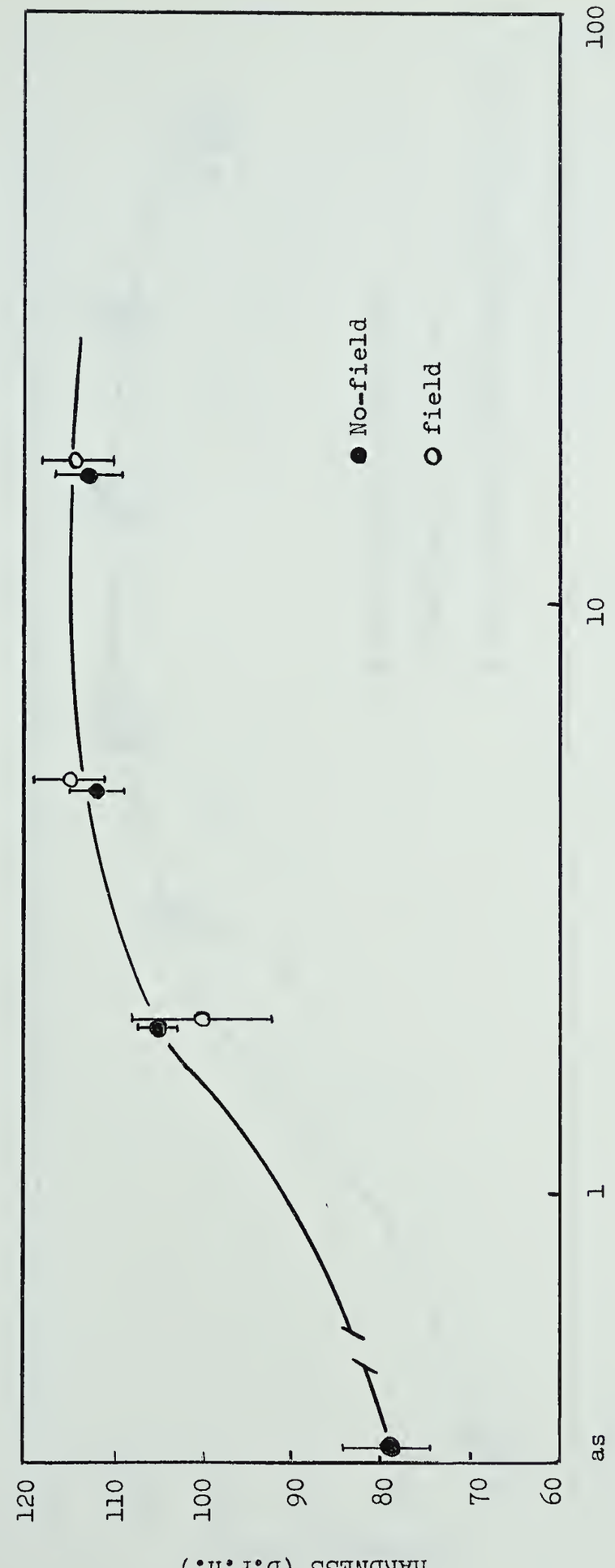

Figure 21. Unworked Al-4.67%Cu alloy aged at 190°C. (Appendix I, N.)

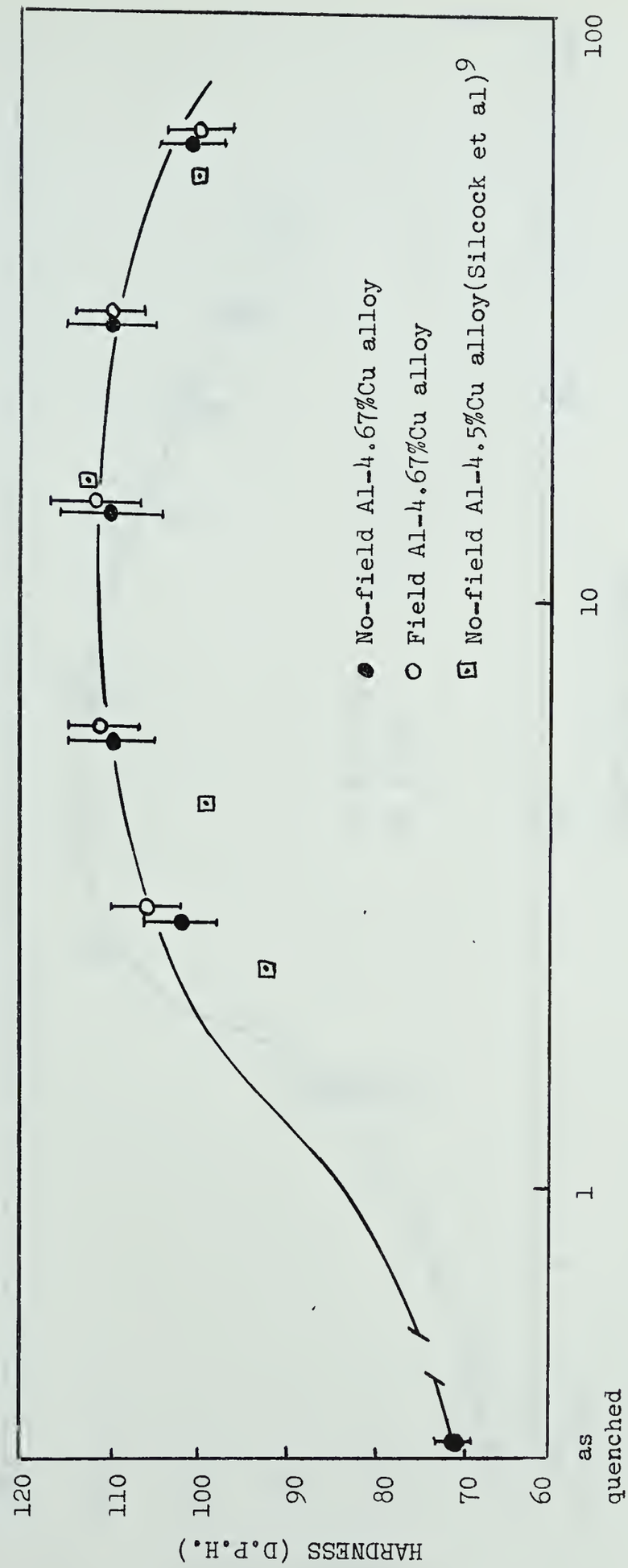

Figure 22. Unworked Al-4.67%Cu alloy aged at 190°C. (Appendix I, P.) Also showing ageing results obtained by Silcock et al[9] for Al-4.5%Cu alloy at 190°C.

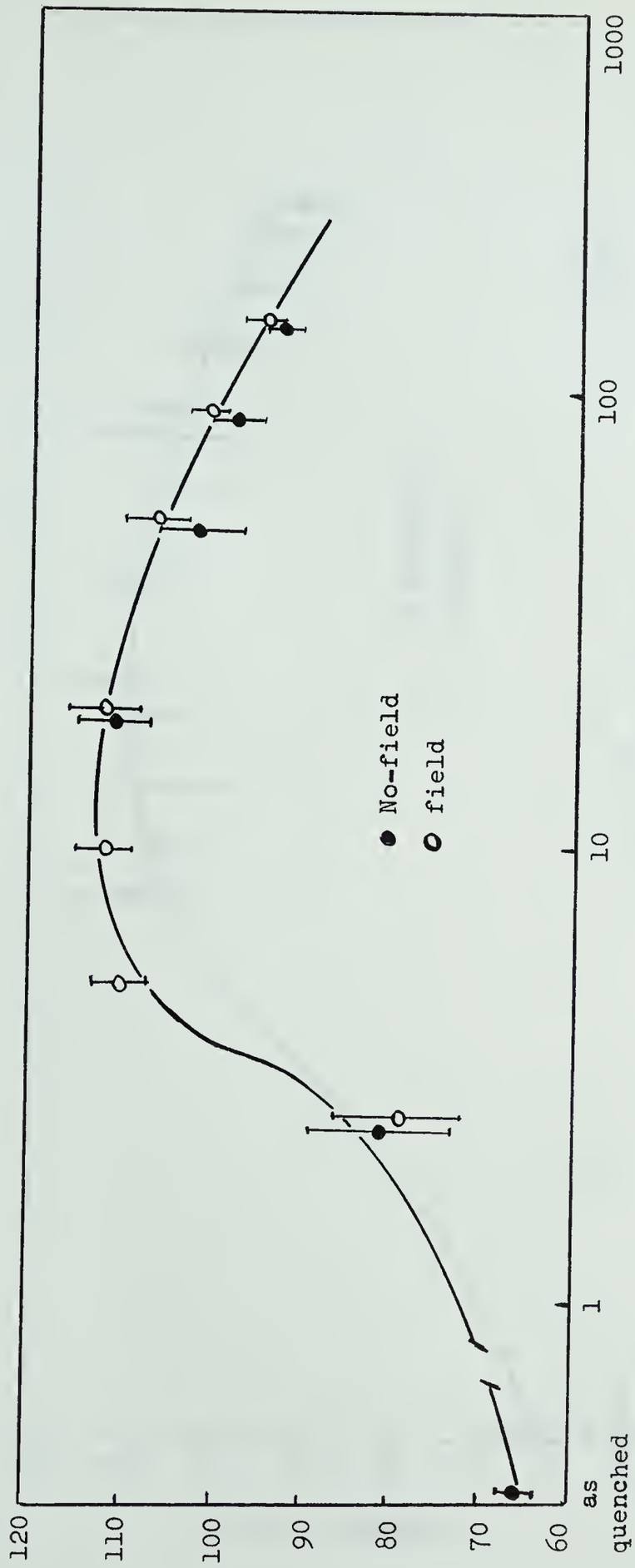

Figure 23. Unworked Al-4.1%Cu alloy aged at 190°C. (Appendix I, Q.)

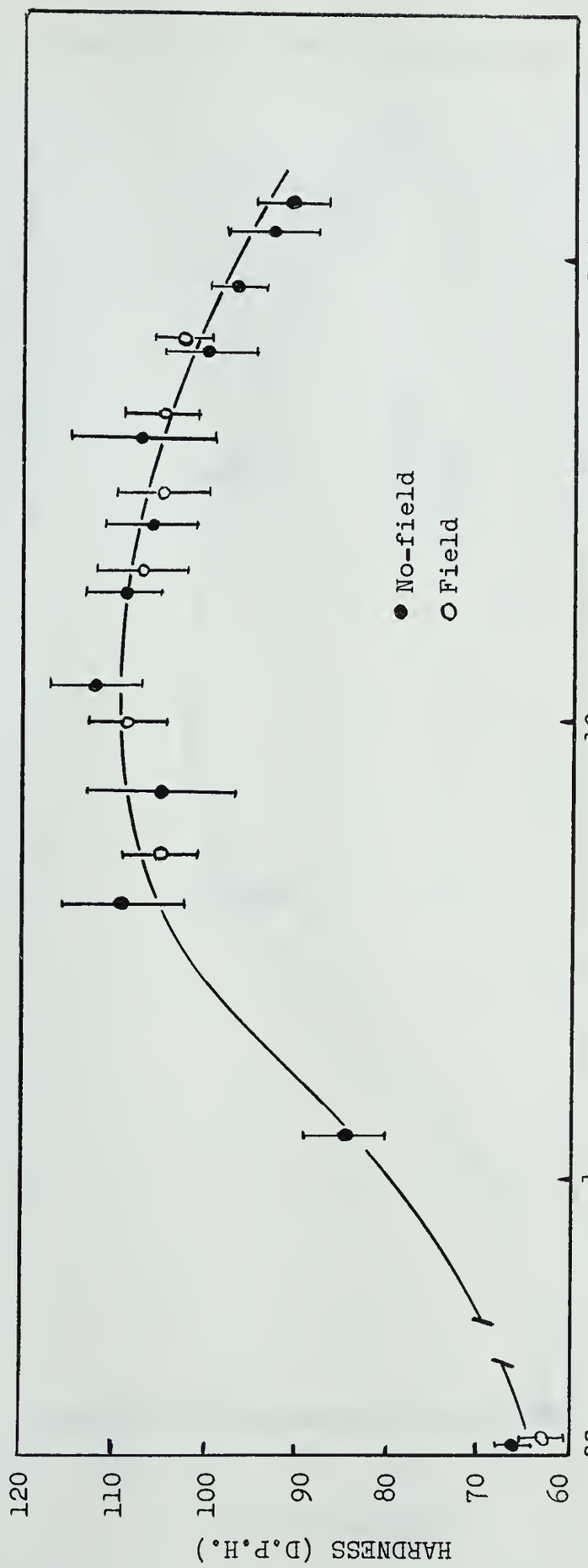

Figure 24. Unworked Al-4.05%Cu alloy aged at 190°C. (Appendix I, R.)

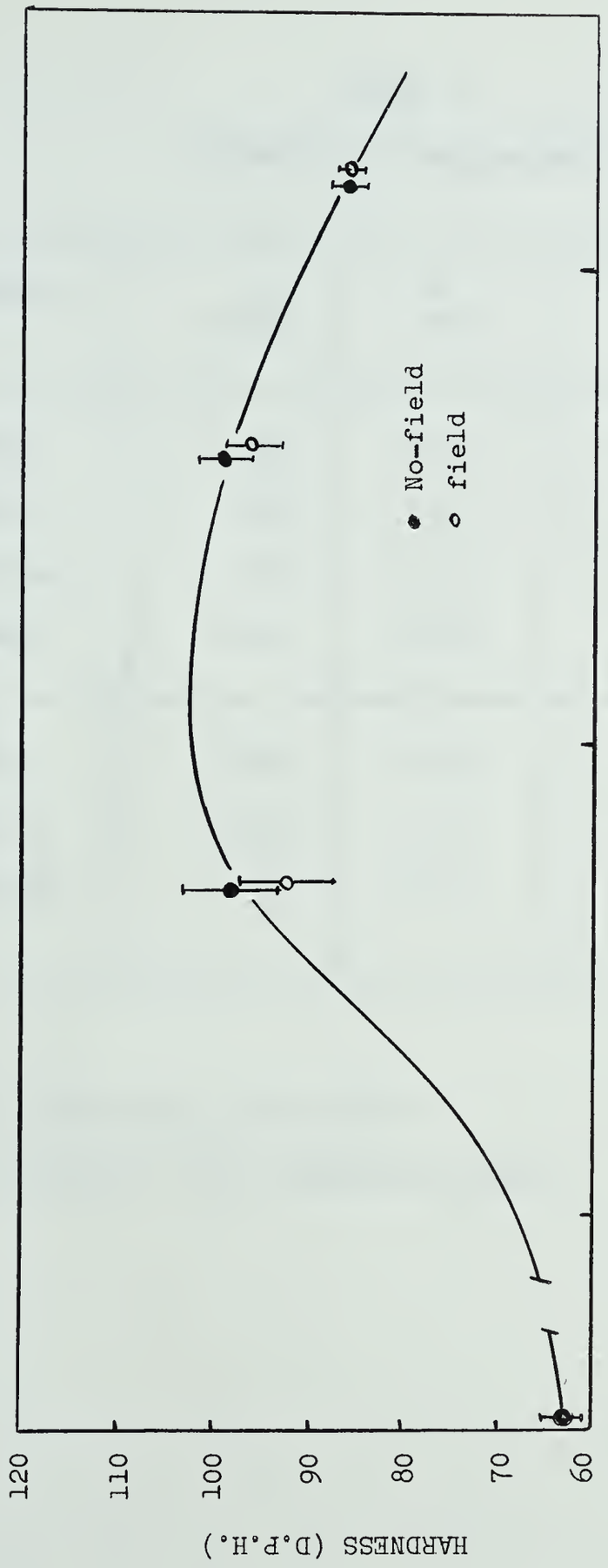

Figure 25. Unworked Al-4.0%Cu alloy aged at 190°C. (Appendix I, S.)

TABLE I

SUSCEPTABILITY MEASUREMENTS

	Specimen	A sq.cm.	Δw mg.	Ak 10^{-6}	k 10^{-6} emu.
*	S.Soln.	0.205	+6.5	+0.28	+1.37
	Max.Hds.	0.207	+7.8	+0.34	+1.64
	Over Agd.	0.203	+8.2	+0.36	+1.77
	θ-phase.	0.214	-0.4	-0.02	-0.09
**	S.Soln.	0.199	+9.4	+0.40	+2.01
	Max.Hds.	0.200	+7.9	+0.34	+1.70
	Over Agd.	0.207	+15.7	+0.68	+3.29

*Al-4.5%Cu alloy, purity 3X9s.

**Al-4.7%Cu-Si alloy, commercial purity.

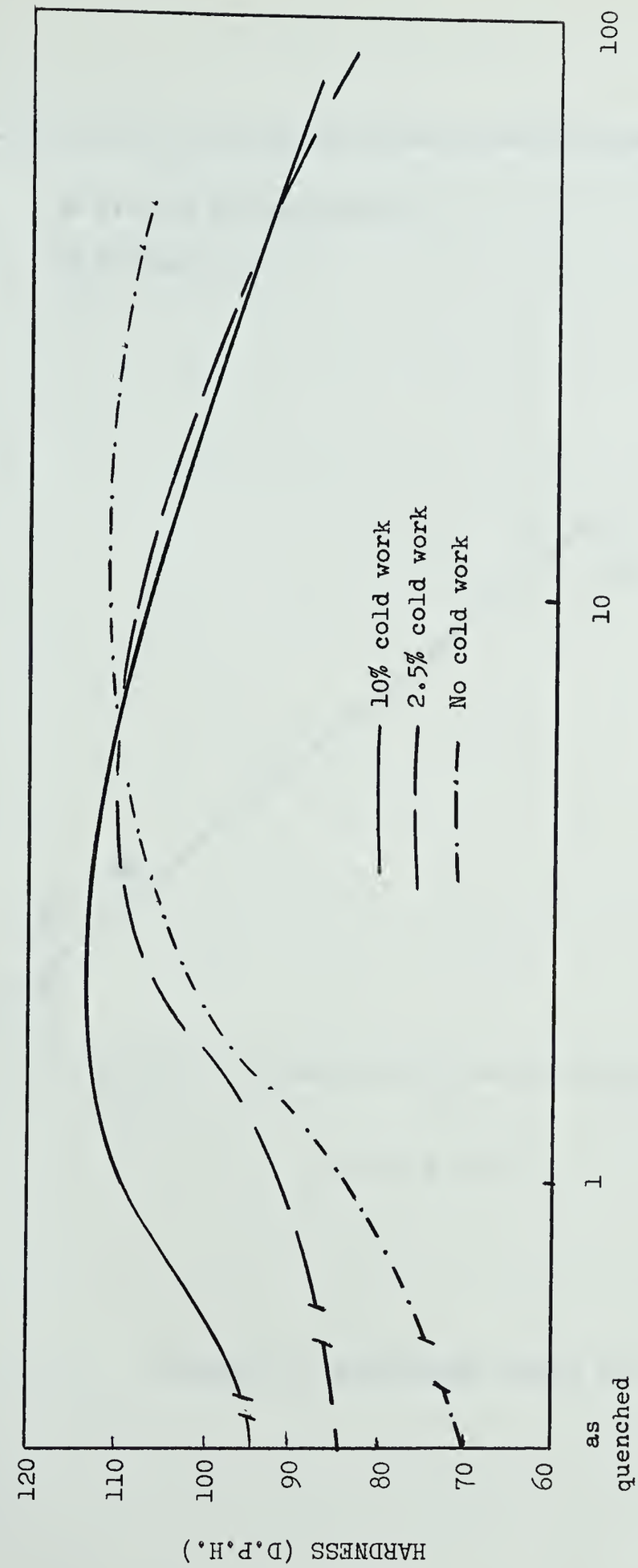

Figure 26. Al-Cu alloys aged at 190°C for varying degrees of cold work. Copper content about 4.7%. (Appendix I, L, M, and P.)

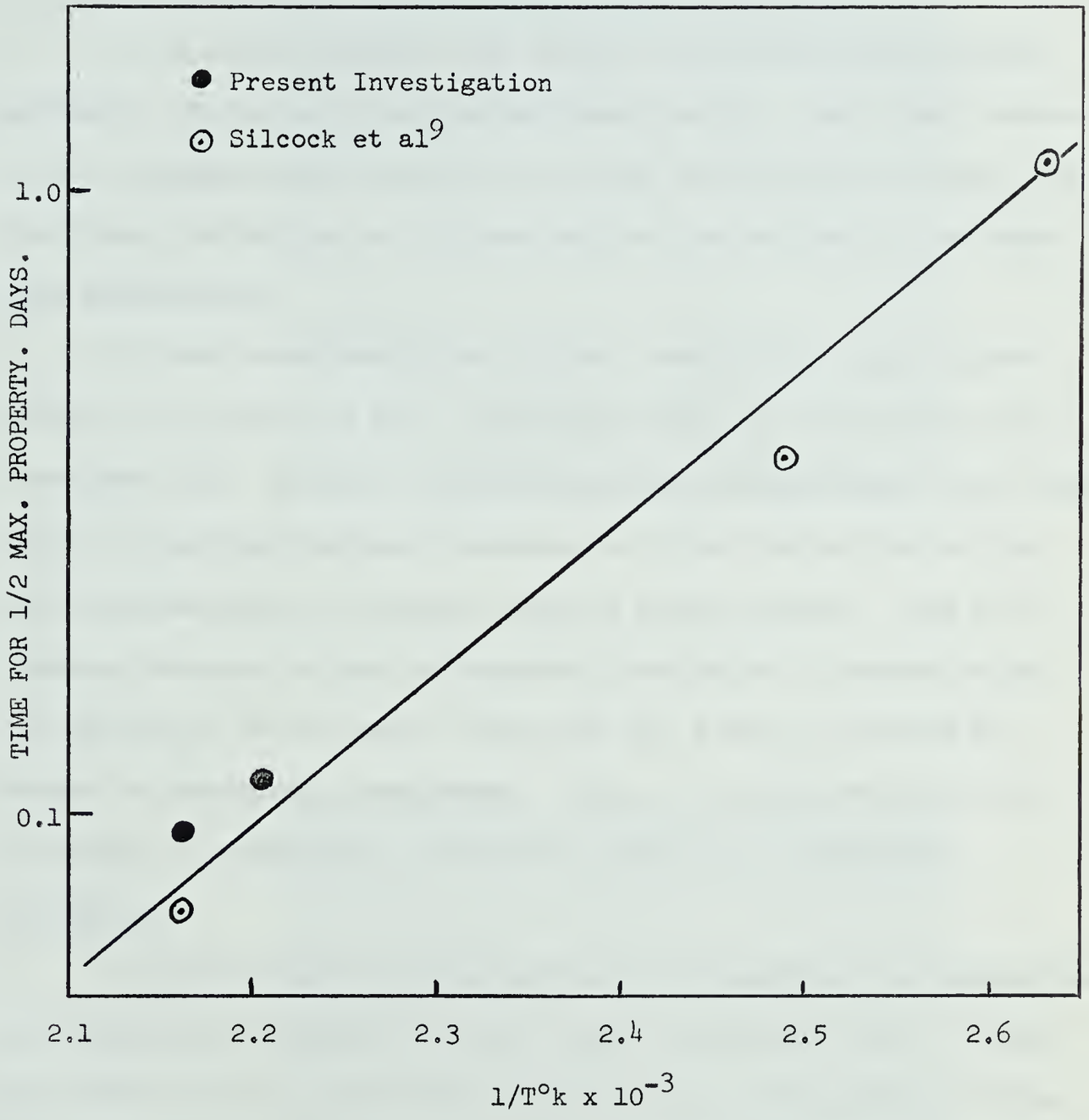

Figure 27. Activation Energy Plot.

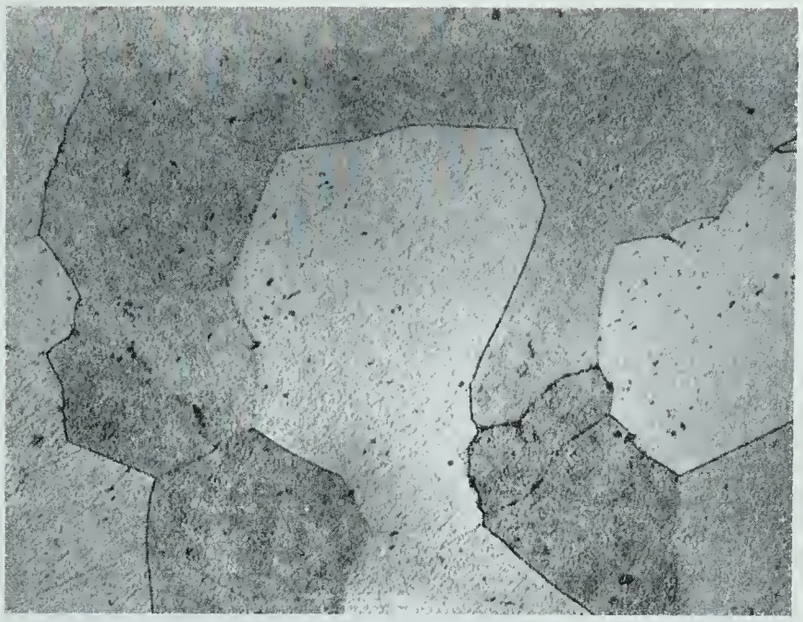

Figure 28 - Al-4.0%Cu alloy in the solid solution state. X200.

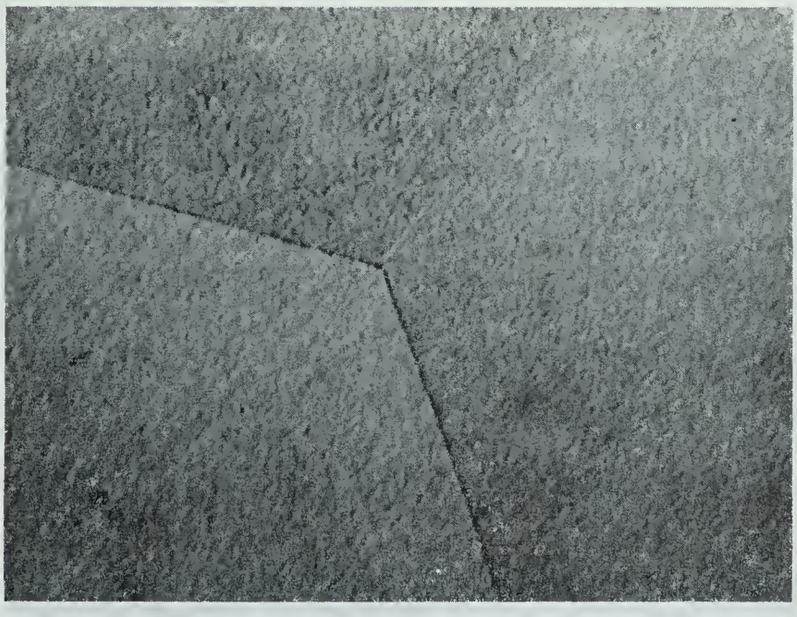

Figure 29 - Al-4.0%Cu alloy in the solid solution state. X1300.

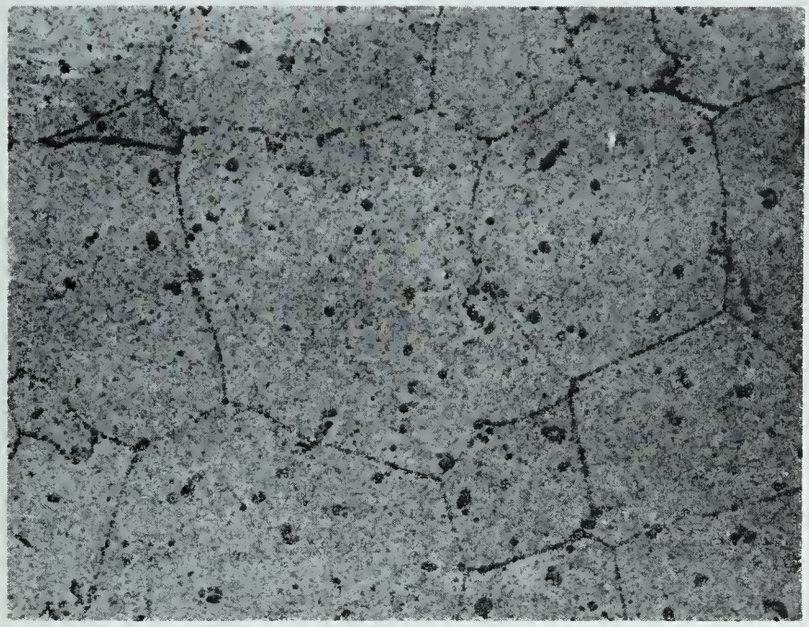

Figure 30 - Al-4.0%Cu alloy aged 5 hours at 190°C.
No-field. X200.

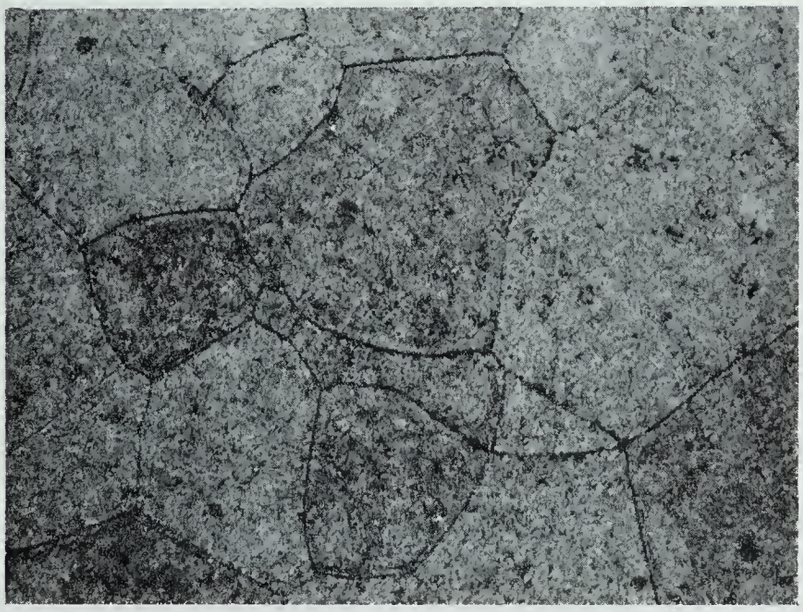

Figure 31 - Al-4.0%Cu alloy aged 5 hours at 190°C.
Field. X200.

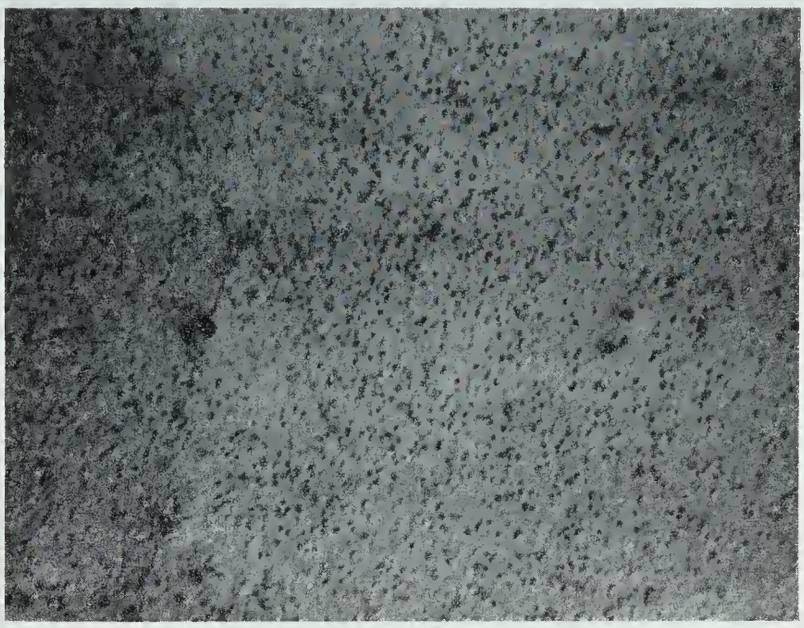

Figure 32 - Al-4.0%Cu alloy aged 5 hours at 190°C.
No-field. X1300.

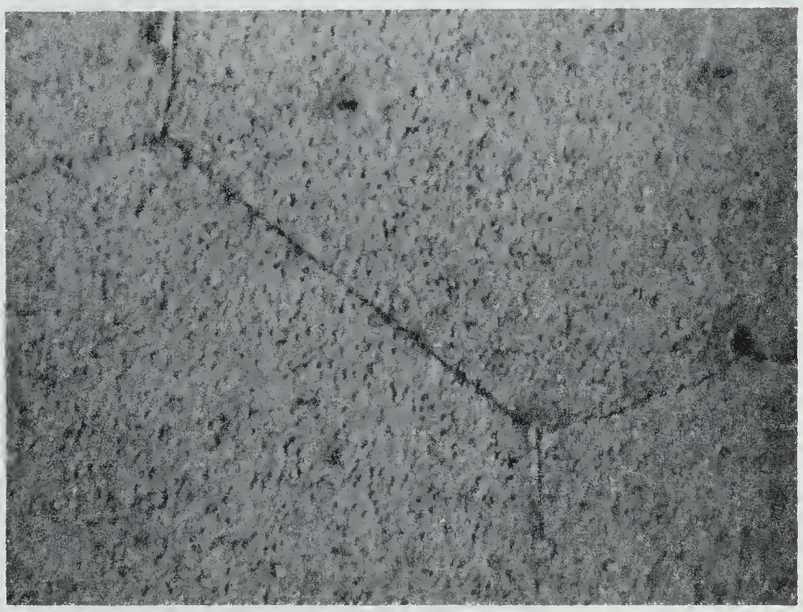

Figure 33 - Al-4.0%Cu alloy aged 5 hours at 190°C.
Field. X1300.

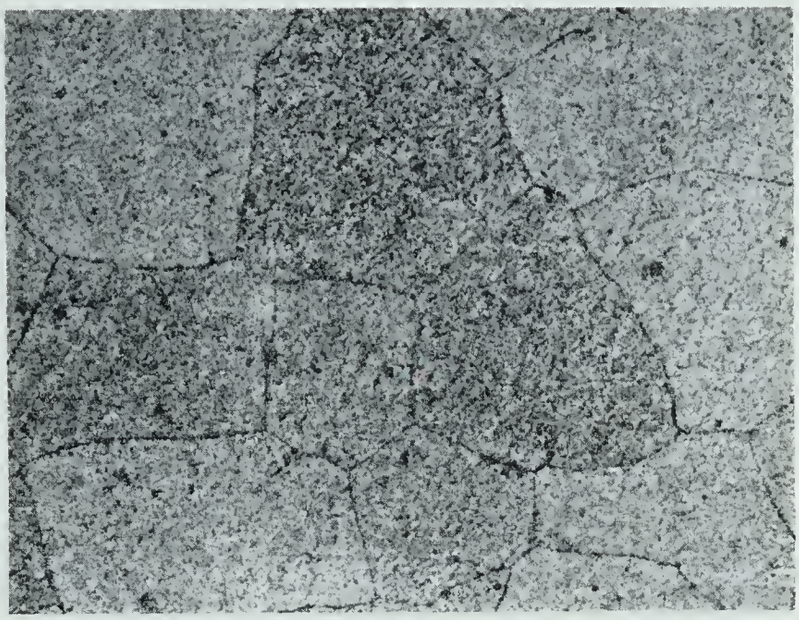

Figure 34 - Al-4.0%Cu alloy aged 155 hours at 190°C. No-field. X200.

Figure 35 - Al-4.0%Cu alloy aged 155 hours at 190°C. Field. X200.

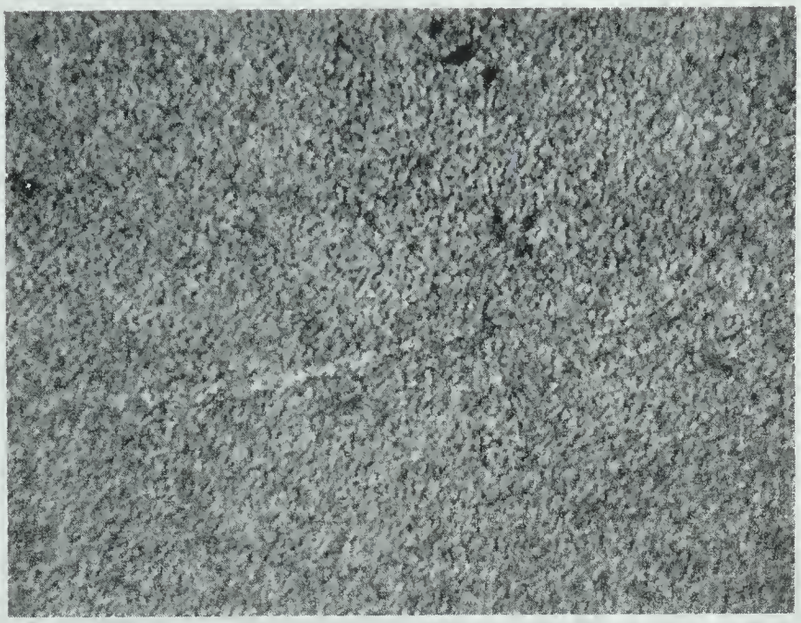

Figure 36 - Al-4.0%Cu alloy aged 155 hours at 190°C.
No-field. X1300.

Figure 37 - Al-4.0%Cu alloy aged 155 hours at 190°C.
Field. X1300.

DISCUSSION OF ERRORS

I. INHOMOGENIETIES OF COMPOSITION

It is highly unlikely that composition errors contributed any systematic variation to the hardness measurements. The copper content of all specimens was evaluated by an X-ray fluorescence technique, the test being carried out on the same surface that was used in the hardness measurements.

For most experiments the specimens were halved along a plane through the cylindrical axis. Hardness values for field and no-field treatments were obtained from corresponding semi-specimens, care being taken to place the hardness indentations on the flat portion of the half-specimens which originally formed a single surface. None of the hardness traverses showed any systematic variation in hardness along the surface of the specimen, indicating that along the surface the sample was essentially homogeneous. Thus, it is concluded that the difference in composition between the halves of a specimen was negligible.

In other experiments the specimens were paired off by composition, the composition variation in a pair never exceeding 0.02%Cu. Paired specimens were aged in and out of the field for equal periods of time. The small variation in copper concentration does not incur a significant hardness error within the limit of the measuring accuracy.

II. TEMPERATURE CONTROL AND MEASUREMENT

The specimens were aged at a constant temperature, subject to a small ripple of $\pm 0.5^{\circ}C$ arising from the on-off action of the controllers.

The mean specimen temperatures were measured on a potentiometer and reproduced to an accuracy of $\pm 0.2^{\circ}C$. Errors in the cold junction temperature were considered negligible since the vacuum flasks were frequently filled and packed in the same manner with crushed ice. The thermocouples were calibrated against a standardized Platinum-10%Rhodium thermocouple by embedding both thermocouples in a silver block and heating this in a furnace. The thermocouples were placed with their junctions about 2 mm. apart, thus ensuring that the temperatures in the region of the junctions were identical. Both field and no-field thermocouples read about $1.5^{\circ}C$ low at $190^{\circ}C$ (see Appendix IV, Table V). Thus the possibility of a temperature difference arising from inhomogeneities of composition between the field and no-field thermocouples is negligible. Variations in room temperature occasionally imposed a drift on one of the controllers, so that over a period of 24 hours the specimen temperature could wander by $1^{\circ}C$ or $2^{\circ}C$. However, the temperatures were checked with considerable frequency and the drift was usually detected and arrested before it went beyond $0.5^{\circ}C$. These drifts were quite infrequent and irregular, adding no systematic error to the ageing process.

Loscoe and Mette[30] have reported that a magnetic field can cause variations in the e.m.f. of the Cromel-P-Alumel thermocouples at ambient temperatures. The variations were produced in the section of the wires subject to a temperature gradient in a magnetic field and not in the junction. Two distinct magnetovoltages were identified, the IDF (independent of field direction) and the DDF (dependent on field direction) voltages. The IDF is proportional to the largest temperature difference between portions of the wires within the field. In the present experiment

about 1" or 1 1/2" of the thermocouple wires were within the field and in this region of the furnace the temperature gradient was about 0.5°C/inch. The thermocouple wires were threaded through silica insulators which minimized the temperature gradient further and it is unlikely that any appreciable IDF voltage was generated. Loscoe and Mette found the IDF magnetovoltage to be a negligible 2uv at 210°C. The DDF depends on the heat gradient <u>across</u> the thermocouple wires. This magnetovoltage can generate an error of 0.25°C for a temperature gradient of 10°C/cm. along the diameter. The thermocouple wires used were 0.012" in diameter. For a temperature gradient of 10°C/cm. to occur it would be necessary for the temperature difference across the wires to be about 0.1°C. Since the wires were extremely thin and were contained in a silica insulating tube kept away from the walls of the furnace it is unlikely that such a temperature difference was generated. Colton[3] investigated this effect at 540°C using a thermocouple arrangement similar to that used in the present experiment and found that the magnetic field had no effect to the thermocouple output. In the present experiment it was found that switching the magnet current on and off had no effect on the measured e.m.f. at 190°C. Thus it is concluded that any magnetovoltages generated were negligible and did not effect the temperature control and reproduceability.

In an attempt to establish the possible temperature variations within the specimen the heat gradient in the central 6" of the furnace was measured. Within the central 2" of the empty furnace the temperature variation was found to be about 1°C (see Appendix V, Figure 39). The specimens were positioned in this region. The distance between the

junction of the measuring thermocouple and the furthest portion of the specimen was about 1 cm. With the temperature gradient found, the temperature difference between the thermocouple junction and the extreme end of the specimen or between opposite ends of the samples would be about 0.2°C. However, the specimens were either wrapped in aluminum foil or placed in a covered alloy vessel and heat conducted along the foil, the vessel and the specimen itself would reduce the temperature gradient considerably. It is unlikely that a temperature difference greater than 0.1°C occurred. In one experiment (Figure 23) several specimens were aged together inside the alloy vessel. The temperature difference between the furthest specimen and the thermocouple junction could have been about 0.2°C in this instance. However, the ageing curve obtained was found to be consistent with other curves, indicating that the existing temperature discrepancy was not sufficiently large to affect the ageing rate.

III. HARDNESS MEASUREMENTS

The amount of room temperature ageing occurring while the specimens were polished and tested for hardness was minimal. Figures 13 and 14 indicate that the maximum rate of room temperature ageing is about 0.4 D.P.H. per hour. The time taken in polishing and testing a specimen was about 20 minutes and in all cases care was taken to ensure that field and no-field specimens were outside of the furnace for identical periods of time. The three minutes chemical polish at 90°C could have induced some ageing, but field and no-field specimens were subjected to identical polishing times. The constancy of the polishing process also ensured that all specimens were polished to the same finish.

Mechanical polishing conditions could not be reproduced with the same constancy as chemical polishes. However, the specimens were highly polished before solution heat treatment and only needed light re-polishing after ageing. The specimens were polished for approximately equal lengths of time on a Buehler Microcloth lap using 0.05 micron alumina abrasive. This was intended to minimize the possibility that unequal mechanical polishing conditions would cause different degrees of work hardening. Errors of this nature were considered insignificant since mechanically polished specimens were not markedly harder than the ones polished chemically, showing that the work hardening effect of polishing was very small.

Hardness values were found to vary noticeably between different indentations on one specimen. This was thought to arise from three main causes:

(1) effects due to grain boundaries and crystallographic orientation.

(2) effects due to the presence of impurities in the indented region.

(3) mechanical effects due to small variations in the cycle of operation of the Tukon tester.

No effort is made to isolate these three errors. Instead diagonal measurements were obtained from indentations made along traverses in a representative central section of the specimen, and the results were treated statistically. For each specimen a mean hardness related to a standard deviation of about 3% to 5% was obtained.

To minimize mechanical errors the testing machine was allowed to warm up thoroughly for over five minutes before hardness measurements

were taken. The first indentation was arbitrarilly discarded to avoid any erroneous results arising from the specimen 'settling down' on the base plate.

IV. SUSCEPTIBILITY MEASUREMENTS

The magnetic field used in the Gouy balance was found to vary slightly from day to day, as is shown by the two calibrations performed on different days. This was due to diurnal variations in the d.c. power supply of the laboratory and the field is assumed to have remained constant during the period of four hours in which the susceptibility measurements were taken and a precise calibration performed.

Due to the limitations of the balance all measurements of magnetic forces suffer an error of about 0.1 mg. The calibration curve was drawn as the best straight line passing through the origin, consistent with the calibration points. This graphical representation would introduce an error estimated to be equivalent to 0.1 mg. Thus, considering the measurements of magnetic forces on the calibrating samples and the calibration line to be exact, an error of ± 0.3 mg. may be attributed to the measurements of magnetic forces of the alloys. This gives an error in the susceptibility results in the region of $\pm 0.01 \times 10^{-6}$ e.m.u.

Errors due to residual magnetism were considered insignificant. Measurements were taken at least three minutes after the field was de-energized and after this interval residual magnetism was negligibly small (see Figures 41 and 42).

DISCUSSION OF RESULTS

I. EFFECT OF PURITY ON AGEING RATE

A noteable result obtained in this investigation was the extremely slow rate of age hardening observed in Al-3.6%Cu alloys made from high purity metals (5X9s pure Al and 6X9s pure Cu). A specimen aged at 180°C increased in hardness by 10 D.P.H. over a period of 45 hours and a sample aged at 300°C actually decreased in hardness after 18 hours (see Figure 15). However, these changes cannot be considered too significant since the measuring errors were quite large by comparison with the magnitude of the changes. The ageing rates were considerably faster for alloys made from medium purity metals (3X9s pure) and were comparable to published data (see Figure 22). Thus the slow precipitation in the high purity alloys was attributed to the scarcity of impurity particles which act as heterogeneous nucleating points. The rate of precipitation of the high purity alloy is thought to be controlled mainly by the rate of homogeneous nucleation; alloys aged at 24°C and 180°C showed no significant difference in ageing rates even though diffusion rates at these temperatures vary by several orders of magnitude. The specimen aged at 300°C showed a tendency to soften on ageing. This may be explained in terms of the very high diffusion rate existing at this temperature combined with the slow rate of nucleation. The few precipitate particles which did nucleate grew very quickly to beyond their optimum size under the accelerated diffusion, thus softening the alloy on the whole.

The influence of nucleating points on the ageing rate was further investigated in the ageing of alloys which had been cold worked in the

solid solution (heat treated) state. Cold work creates a large number of dislocation clusters and lattice strains which will act as nucleation points and accelerate precipitation. This is evident from Figure 26 which shows that the rate of ageing increases with the degree of cold work. Cold work introduces strains into the alloy and the cold worked samples were found to have a higher solid solution hardness than the unworked material. These mechanical strains were largely released after a few hours at 190°C since unworked and 10% cold worked specimens attained the same maximum hardness.

II. EFFECT OF A MAGNETIC FIELD ON AGEING RATE

A magnetic field was found to have no noticeable effect on the ageing rate of 99.9% pure alloys, whether cold worked or not. Since the precipitation rate is dependent on nucleation and diffusion, this indicates that the presence of a magnetic field has a negligible effect on diffusion and nucleation rates.

Youdelis et al[4] and Colton[3] have shown that the diffusion rate of Cu atoms in Al-3%Cu is inhibited by 25% in a 34 kilo-oersted field. The inhibition of diffusion was due to Lorentz forces on the electrons, acting in the absence of a Hall field. The diffusion-inhibited electrons slow the diffusion transported ion cores to the same extent through electrostatic forces by virtue of the requirement for charge neutrality. In order for the field inhibition to occur, an electrostatic Hall field must not arise through charge accumulation against bounding surfaces of the sample, otherwise the Lorentz force on the electrons is cancelled. It has been shown that a Hall field will be largely short circuited in a region where the length (l) to width (w)

ratio of the transport zone is greater than three. Youdelis et al measured an l/w ratio of about 10^{-2} in the diffusion-transported zone and concluded that no Hall field was present. In the present experiment the diffusion zone length was about 2.10^{-4} cms. This value was obtained from the dimensions of the copper-depleted region in the neighbourhood of a precipitate particle (see Appendix VII). To a first order approximation the width may be taken as the diameter of a precipitate particle, which is approximately 10^{-5} cm. Thus the l/w ratio is such that a Hall field is generated to cancel out the magnetic inhibition of diffusion. Thus the absence of any magnetic effect on the precipitation rate, acting via the diffusion process, may be explained and substantiated theoretically. Although the possibility of the ineffectiveness of the field in influencing volume diffusion rates for the particular case of solid precipitation was appreciated from the outset, there remained the possibility of the magnetic field exerting an inhibiting influence on "short cut" diffusion mechanisms such as diffusion along dislocation lines, grain boundaries and other crystal lattice defects. "Short cut" diffusion paths have been postulated to account for the high transformation rates in precipitation reactions, which otherwise could not be explained on the basis of known volume diffusion rates. It is clear from the results of the present investigation that if "short cut" diffusion mechanisms occur in the Al-Cu system, they are unaffected by the magnetic field.

However, diffusion is not the only effect influencing nucleation. The very slow ageing rate observed in the high purity alloys and the accelerated ageing which occurred in cold worked alloys suggest that

the nucleation rate has a predominant effect on the ageing rate. It has been shown earlier that a change of phase in a magnetic field could give rise to an energy term if a change in susceptibility accompanied the reaction. The magnetic energy, ΔG_M, was introduced explicitly into the nucleation rate equation (see Equations 8 and 9), and the magnetic energy is given by $1/2(\chi_\beta - \chi_\alpha).H^2$. The magnetic field will have a noticeable effect on the nucleation rate only if ΔG_M is comparable to ΔG_{NM}, the non-magnetic activation energy. Fine and Chiou[5] calculated the activation energy for precipitation in Al-Cu alloy to be about 12 to 14 K.cal/mole. Turnbull et al[32] and Freidel[33] estimated the activation energy to be slightly lower, about 10 K.cal/mole and 9 K.cal/mole respectively. Using results obtained in this investigation and data published by Silcock et al[9] the activation energy was calculated using the method of Robertson et al.[34] Figure 27 shows a plot of "Time for 1/2 maximum property" against $1/T$, where T is the temperature in degrees Kelvin. The "Time for 1/2 maximum property" was taken as the ageing time required to reach a hardness of 1/2(maximum hardness - as quenched hardness). The rate of reaction is given by an equation of the form

$$\text{Rate} = 1/t = B.\text{Exp}-(Q/RT).$$

where t is time, Q is the activation energy, and B is some constant. Thus,

$$\frac{\ln t}{1/T} = \frac{\ln(1/B)}{1/T} + \frac{Q}{R}.$$

In practice the graph lnt Vs. 1/T is a straight line of slope Q/R. Thus from Figure 27 the activation energy, Q, was calculated to be 11.8 K.cal/mole.

In Al(rich)-Cu alloys the susceptibility was measured at $1.37X10^{-6}$ e.m.u. for the solid solution state and $1.77X10^{-6}$ e.m.u. for the

overaged condition. This susceptibility change gives rise to an energy change ΔG_M of 10^{-4} cal/mole, which is clearly insignificant in comparison with the normal precipitation activation energy of about 12 K.cal/mole. Thus theoretical considerations do not predict a magnetic effect on the nucleation rate, which is consistent with experimental results. It was suspected that the susceptibility differences involved might not contribute a significant magnetic energy term in the expression for the nucleation rate, thus leaving the ageing rate as a whole unaffected by the field. However, there still remained the possibility of the magnetic polarization of the activated state (during the formation of a zone) facilitating or inhibiting the nucleation process. Results of this investigation indicate little or no effect of the field on the activated states of the atoms forming the clusters or zones.

The susceptibility of the alloy containing 0.8% Si was slightly higher than that of pure aluminum-copper alloy. This was attributed to the strong paramagnetic susceptibility of the silicon metal. Figure 16 shows that the overageing rate was slightly faster in the field. The change in susceptibility from $2.01X10^{-6}$ (solid solution) to $3.27X10^{-6}$ e.m.u. (overaged) only represents a magnetic energy component of about $3X10^{-4}$ cal/mole. This is unlikely to have caused any variation in the nucleation rate and the faster overageing of the field samples is considered to be an erroneous result arising from an undetected temperature discrepancy.

Figures 28 to 37 show the change in structure in an Al-4.0%Cu alloy during ageing. At a magnification of X200 grain boundary structure is clearly seen, but the resolution is not sufficiently fine

to identify the precipitate. No difference in grain size was found between field and no-field cases. Indeed, there was no indication of a change in grain size as ageing progressed. The photomicrographs taken at X1300 show a marked contrast between the overaged alloy (155 hours) showing abundant precipitate and the precipitate-free solid solution alloy. After 5 hours ageing at 190°C the alloys show evidence of a small amount of precipitate. In all cases field and no-field specimens exhibit similar characteristics and no difference in size or quantity of precipitate may be observed. This substantiates the experimental hardness results and the theoretical conclusions that a magnetic field has a negligible effect on the precipitation behaviour of Al(rich)-Cu alloys.

SUMMARY AND CONCLUSIONS

1. Extremely high purity alloys (5X9s) exhibited very slow ageing rates. This was attributed to the scarcity of impurity particles which act as nucleation points.

2. Alloys of medium purity (3X9s) showed ageing rates comparable to published data. Cold working of the alloys in the solid solution state resulted in an accelerated ageing rate due to the formation of numerous nucleation points in the form of dislocation clusters and strained regions in the lattice.

3. The ageing rate in a magnetic field was found to be the same as in the no-field case, both for cold worked and unworked alloy.

4. Theoretical considerations show that the dimensions of the diffusion region in the neighbourhood of precipitate particles are such that no inhibition of diffusion is predicted due to the existence of a Hall field.

5. On the basis of experimental results it is assumed that "short cut" diffusion mechanisms are not affected by a magnetic field.

6. Magnetic energies arising from a susceptibility change during precipitation are in the order of 10^{-4} cal/mole. This energy is minute in comparison to the precipitation activation energy of 12 K.cal/mole, and it is concluded that a magnetic field does not affect the nucleation rate in Al(rich)-Cu alloys. It is also inferred that the activated state remains magnetically unpolarized and has no effect on the overall ageing rate.

7. Photomicrographs give no indication that the morphology of the aged alloy is affected by a magnetic field. More specifically, the $CuAl_2$ precipitate exhibits no anisotropy in a magnetic field.

BIBLIOGRAPHY

1. J.B. Newkirk, "Precipitation from Solid Solution", A.S.M. 1959.

2. F.W. Camp and E.F. Johnson. 1961. "Effect of Strong Magnetic Fields on Chemical Engineering Systems", U.S. Atomic energy.

3. D.R. Colton, Ph.D. Thesis, 1964. U of A.

4. W.V. Youdelis, D.R. Colton, and J. Cahoon. Canadian Journal of Physics. 1964 42 2217.

5. M.E. Fine and C. Chiou. AIME Trans. 1958 212 553.

6. J.T. Vietz, K.R. Sargant, and J.J. Polmear. I of M journal. 1963-4 92 327.

7. G.D. Preston.
   Nature. 1938 142 570.
   Proc. Roy. Soc. 1938 (A) 167 526.
   Phil. Mag. 1938 (vii) 26 855.

8. A. Guinier.
   Nature. 1938 142 569.
   Ann. Physique. 1939 (xi) 12 161.
   J. Phys. Radium. 1942 (viii) 3 129.

9. J.M. Silcock, T.S. Heal, and H.K. Hardy. I of M Journal. 1953-4 82 1519.

10. R.E. Smallman. "Modern Physical Metallurgy". Butterworths. 1962.

11. J.R. Cahoon, Masters Thesis, 1963. U of A.

12. W.V. Youdelis, D.R. Colton, and J. Cahoon. Canadian Journal of Physics. 1964 42 2238.

13. W.W. Mullins. Acta Met. July 1964 4 421.

14. V.B. Fiks. Soviet Physics. (S.S.) 1959 1 14.

15. V.B. Fiks. Soviet Physics. (S.S.) 1964 5 Pt. 3 2549.
    Soviet Physics. (S.S.) 1964 6 #6 1251.

16. T.G. Cowling. "Magnetohydrodynamics". Interscience Pub. Inc. 1957.

17. J.S. Kirkaldy, G.R. Mason, and W.J. Slater. Can. Inst. Mining Bull. 1961 54 59.

18. J.B. Murphy. Acta Mat. 1961 9 563.

19. J.S. Kirkaldy and W.V. Youdelis. Trans. AIME. 1958 212 833.

20. W.V. Youdelis and D.R. Colton. Trans. AIME. 1960 218 628.

21. E. Justi. Physikalische Zeitschrift. 1936 37 766.

22. C.D. Graham, Sr., "Mag. Props. of Metals and Alloys" ASM 1958 288.

23. S. Kaya. Review of Modern Physics. 1953 25 49.

24. J.J. de Jong, J.M.G. Smeets, and H.B. Haarstra. Journal of Applied Physics. 1958 29 297.

25. H. Jahn. Die Technik. 1958 Jan/Feb. 13.

26. O. Snellman and F.J. Burge. J. Sci. Inst. 1949 26 331.

27. L.F. Bates. "Modern Magnetism". 1961 p 115.

28. P.W. Selwood. "Magnetochemistry". 1956 p 3.

29. C.J. Smithells. Metals Reference Book. 1962.

30. C. Loscoe and H. Mette. "Temp. Measurement and Control in Science and Industry". 1962 3 Pt. II 283.

31. E.H. Putney. "The Hall Effect and Related Phenomena". Butterworth. 1960 45.

32. D. Turnbull and H.N. Treaftis. Acta Met. 1957 5 534.

33. J. Freidel. "Les Dislocations". 1959 247.

34. W.D. Robertson and R.S. Bray. "Precipitation from Solid Solution". ASM 1959.

General.

35. "The Mechanism of Phase Transformations in Metals". Institute of Metals. #8 1956.

36. V.F. Zackay and H.I. Aaronson. "Decomposition of Austenite by Diffusional Processes". (Interscience Pub.) 1962.

APPENDIX I

EXPERIMENTAL CONDITIONS

TABLE II. DETAILS OF EXPERIMENTAL CONDITIONS RELATED TO THE DIFFERENT AGEING EXPERIMENTS

Expt.	Composition	Purity	Age Temp. °C.	Ageing Method	Polish
A	Al-3.53%Cu	5X9s	20-24	4	Chem.
B	Al-3.58%Cu	5X9s	20-24	4	Chem.
C	Al-4.7%Cu -0.8%Si	comm-ercial	20-24	4	Chem.
D	Al-4.1%Cu	3X9s	20-24	4	Chem.
E	Al-3.6%Cu	5X9s	180	4	Chem.
F	Al-3.61%Cu	5X9s	300	4	Chem.
G	Al-4.7%Cu -0.8%Si	comm-ercial	180	1	Chem.
J	Al-4.63%Cu	3X9s	190	4	Chem.
K	Al-4.96%Cu	3X9s	190	4	Chem.
L	Al-4.77%Cu	3X9s	190	4	Chem.
M	Al-4.68%Cu	3X9s	190	4	Chem.
N	Al-4.67%Cu	3X9s	190	4	Chem.
P	Al-4.67%Cu	3X9s	190	4	Chem.
Q	Al-4.1%Cu $\pm$0.05%Cu	3X9s	190	1	Chem.
R	Al-4.05%Cu	3X9s	190	3	Mech.
S	Al-4.0%Cu	3X9s	190	4	Mech.

APPENDIX II

TREATMENT OF HARDNESS DATA

Hardness values, expressed as D.P.H. (diamond pyramid hardness) were determined by forcing a square base diamond pyramid having an apex angle of 136° into the specimen under a load of 1 K.g. and measuring the diagonals of the indentation produced. The D.P.H. is defined as the load per unit area of surface contact in K.g. per square mm., as calculated from:

$$D.P.H. = \frac{2\,L\,\mathrm{Sin}(a/2)}{d^2} \qquad - - - - \qquad (11)$$

where: d = length of average diameter in mm.

a = 136° apex angle.

L = 1 K.g. load.

The diagonals were measured in terms of filar units in the microscope eyepiece. Using a 6 mm. objective lens the conversion factor was

filar units X 0.258 = microns.

Calibration tables provided by the manufacturers to the Tukon Tester facilitated the calculation of D.P.H. values from measurements of diagonals. Each hardness value was obtained from the average of about 10 or 15 impressions. The standard deviation of each value was calculated from the formula

$$\text{standard deviation, } \sigma = \sqrt{\frac{\Sigma d^2 - (\Sigma d)^2}{N-1}}$$

where N is the number of diagonal measurements.

The hardness values obtained for a representative sample are given as an illustration.

Example:

Specimen aged 3 hours at 190°C after 10% cold work (Table VIII).

Diagonal measurements

Traverses.		
#1	#2	#3
493	485	495
496	494	496
500	492	482
487	485	481
487	500	491
490	498	488
	478	
	479	

N = 20.

Total = Σd = 9797 filar units.

Mean = $\underline{d}$ = 490 filar units.

$\Sigma(d^2)$ = 4799933

$(\Sigma d)^2$ = 4799060

$$)\underline{873}$$
$$41$$

$\sigma = \sqrt{41} = 6.4$.

diameter = 490 ± 6.4 filar units.

= $490 \pm 1.3\%$ filar units.

= $126.4 \pm 1.3\%$ microns.

Hardness = $116 \pm 2.6\%$ D.P.H.

(Note the error is doubled since D.P.H. $\alpha \frac{1}{d^2}$).

Hardness = 116 ± 3 D.P.H.

APPENDIX III

X-RAY DETERMINATION OF COPPER CONTENT

All specimens were analysed on a Phillips X-Ray Fluorescence unit. A calibration was carried out Al-Cu standards with copper contents of 0.86%, 1/79%, 2.78% and 3.67%. X-Rays were allowed to impinge on the specimens for 10 seconds and a measure of the copper content was obtained on a scintillation counting device; the mean of 10 counts was taken.

The analysis carried out for specimens from an ingot of 99.9% purity alloy is presented to illustrate the procedure and the accuracy of the test.

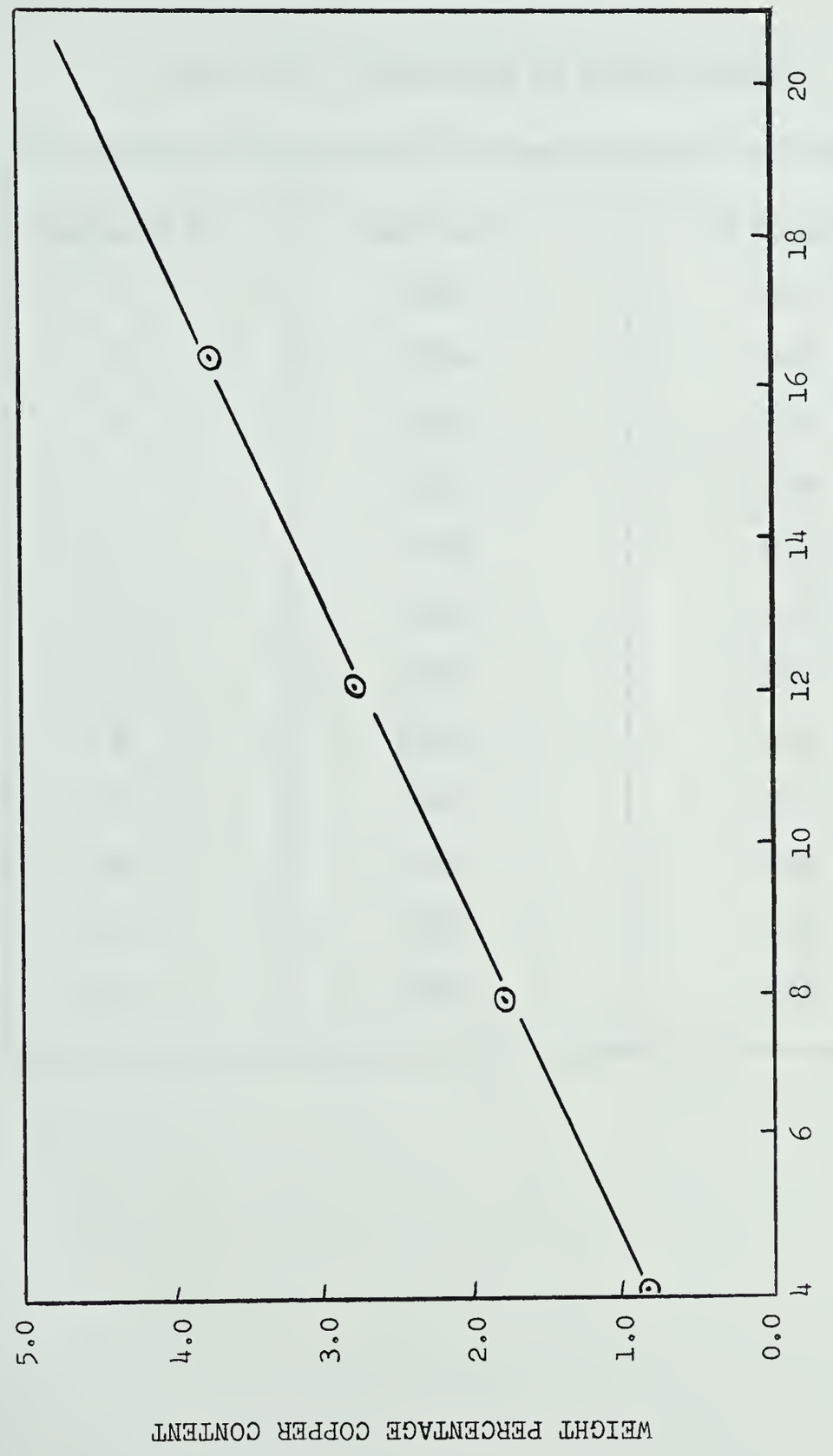

Figure 38. Calibration of Standards

TABLE III. EVALUATION OF COPPER CONTENT

Specimen #.	Mean Count	% Copper.
1	18304	4.05
2	18309	4.05
3	18323	4.05
4	18372	4.06
5	18558	4.10
6	18583	4.10
7	18692	4.13
8	18621	4.11
9	18692	4.13
10	18787	4.15
11	18879	4.17
12	18857	4.16

APPENDIX IV

CALIBRATION OF THERMOCOUPLES

Measuring thermocouples of Cromel-p-Alumel calibrated against a Platinum-10%Rhodium standard. Errors against absolute temperature are reported.

TABLE IV. CALIBRATION OF THERMOCOUPLES

Temperature Range	Error in No-F t.c.°C.	Error in Field t.c.°C.
20 to 24 C	1.0 High	0.5 High
197 to 200 C	1.5 Low	1.5 Low
540 to 550 C	2.8 Low	2.5 Low
690 to 710 C	2.5 Low	2.5 Low
790 to 810 C	2.5 Low	2.5 Low

APPENDIX V

TEMPERATURE GRADIENT OF FURNACE

The temperature gradient in the central six inches of the ageing furnace is shown in Figure 39. Within the central two inches, where the specimen was placed, the temperature variation was in the region of 1°C.

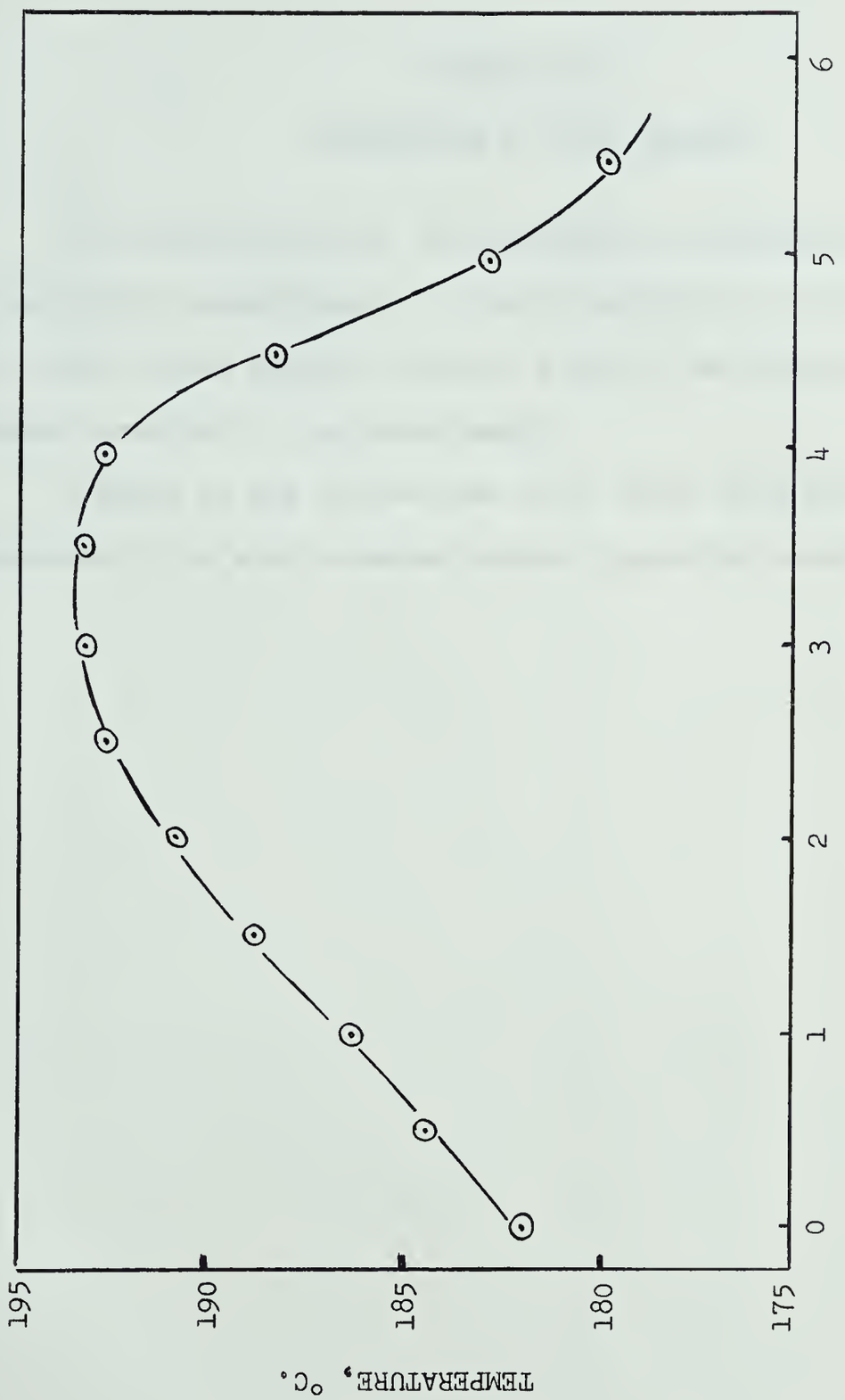

Figure 39. Temperature gradient along central 6" of ageing furnace.

APPENDIX VI

CALIBRATION OF GOUY BALANCE

The main calibration was performed in conjunction with alloy susceptibility measurements. A second calibration carried out at a later date varied slightly from the previous calibration line due to a diurnal variation in the power supply.

Figures 41 and 42 show that after about three minutes residual magnetism in the electro-magnet becomes negligibly small and constant.

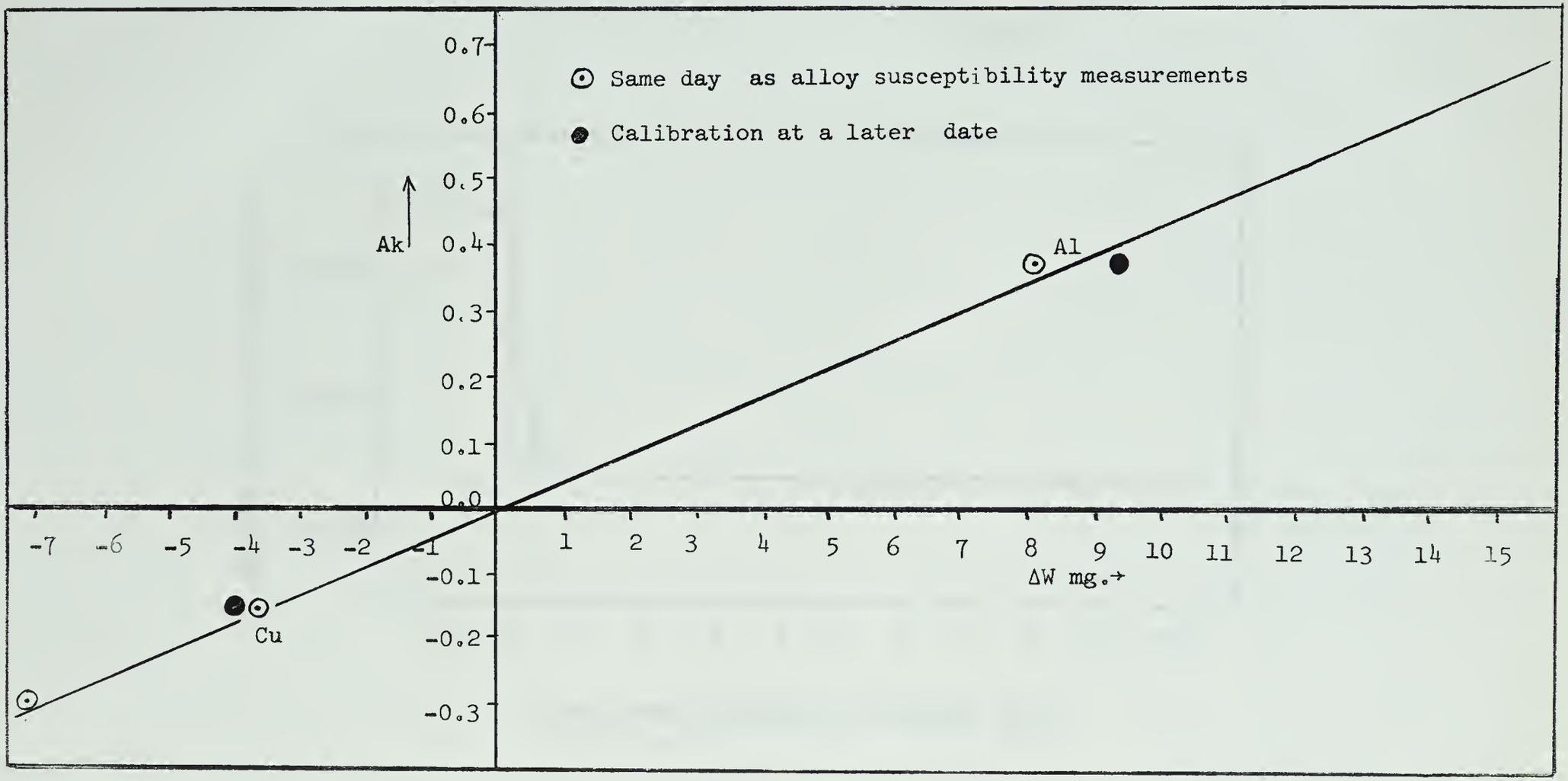

Figure 40. Calibration of Gouy Balance.

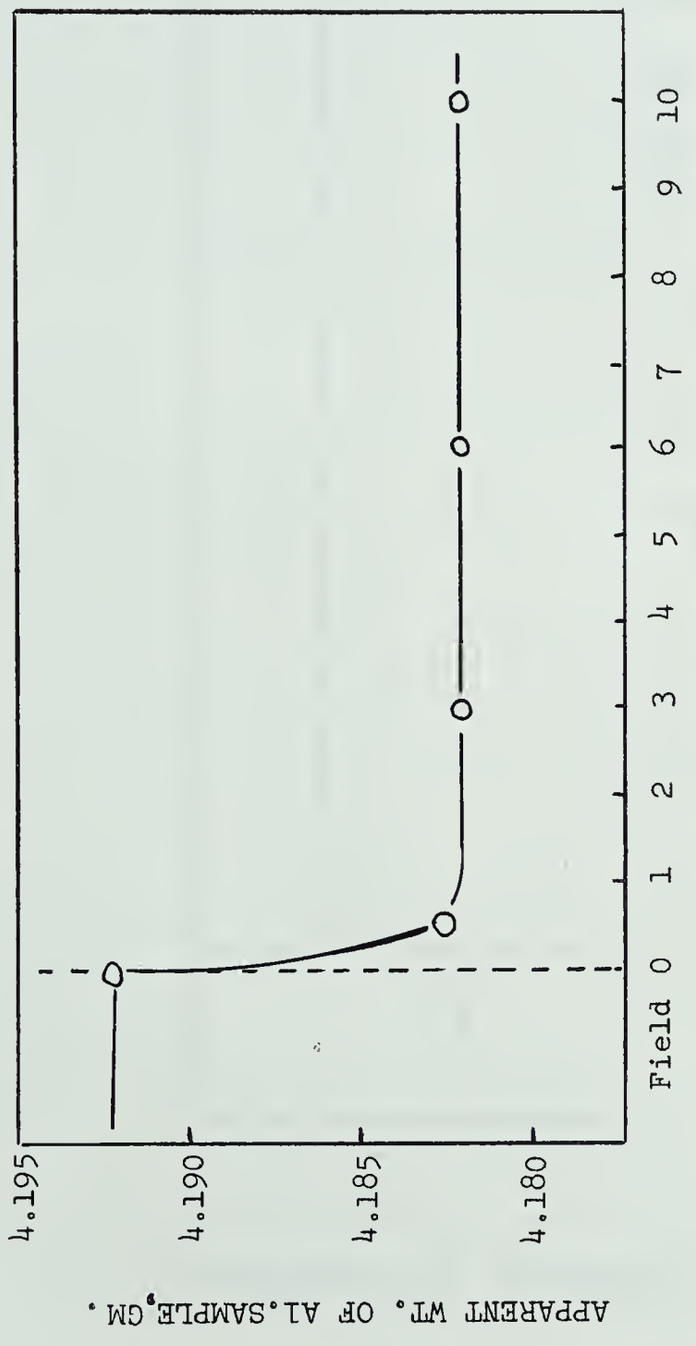

Figure 41. Drop in the effect of residual magnetism in the susceptibility measurement of aluminum.

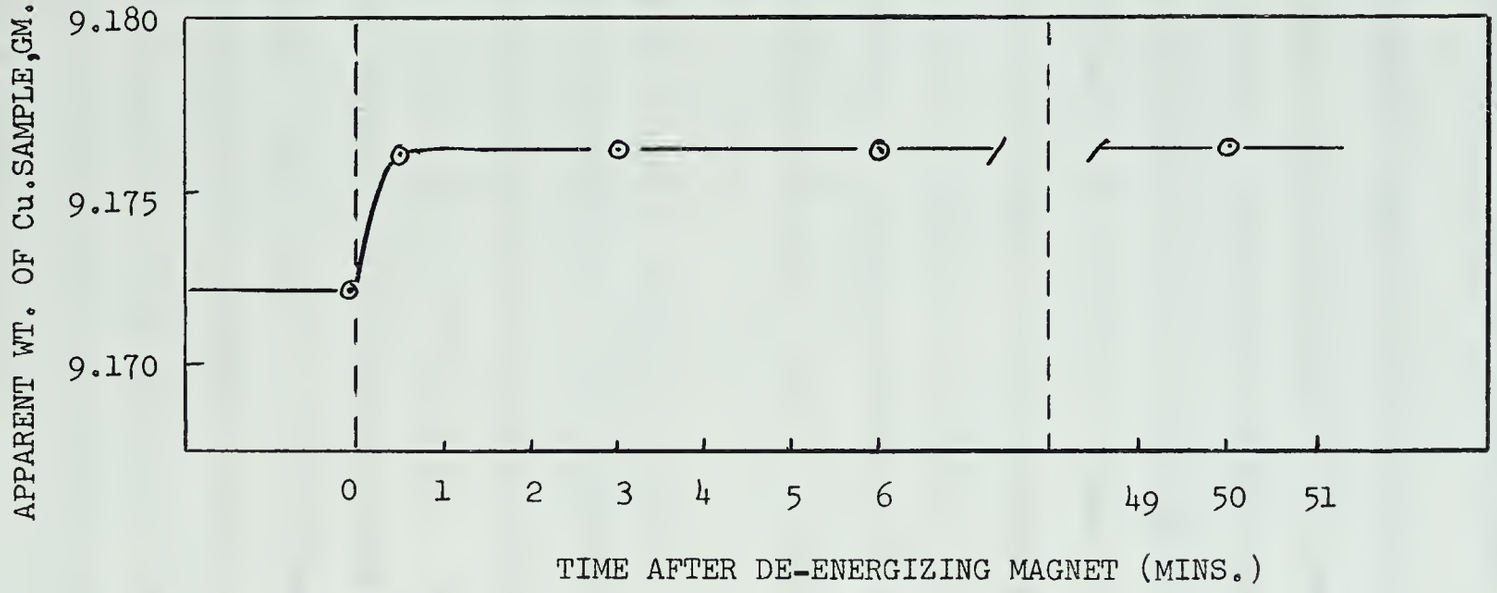

Figure 42. Drop in the effect of residual magnetism in the susceptibility measurement of copper.

APPENDIX VII

CALCULATION OF DIFFUSION ZONE LENGTH

Zackay and Aaronson[36] considered the build up of carbon atoms to form an austenitic region. The formation of the θ precipitate in Al(rich)-Cu alloys involves a depletion of copper atoms from the solid solution to form the precipitate particle, and may be treated in the same manner as the formation of austenite. Figure 43 shows the copper concentration profile in the region of the advancing precipitate/matrix boundary. Copper atoms are depleted from region A to form the precipitate concentration build up B. Thus the areas A and B may be equated. The area A may be considered as triangular to a good approximation, giving the equation

$$x.(C_\theta - C_{sl}) = 1/2(C_{ss} - C_{sl}).\Delta x$$

where C_θ is the copper concentration in the θ-phase, C_{sl} is the copper concentration at the solubility limit at 190°C, and C_{ss} is the nominal copper concentration in the solid solution state. The growth of the precipitate along the x-direction is given by x, and Δx gives a measure of the diffusion depleted zone, which is the diffusion zone length.

Concentration values may be obtained from the Cu-Al equilibrium diagram: C_θ = 33 At.%, C_{sl} = 0.1 At.%, and C_{ss} = 2 At.%. The precipitate particles are lenticular with diameter about 10^3Å and thickness about 10^2Å; x is taken as 10^3Å.

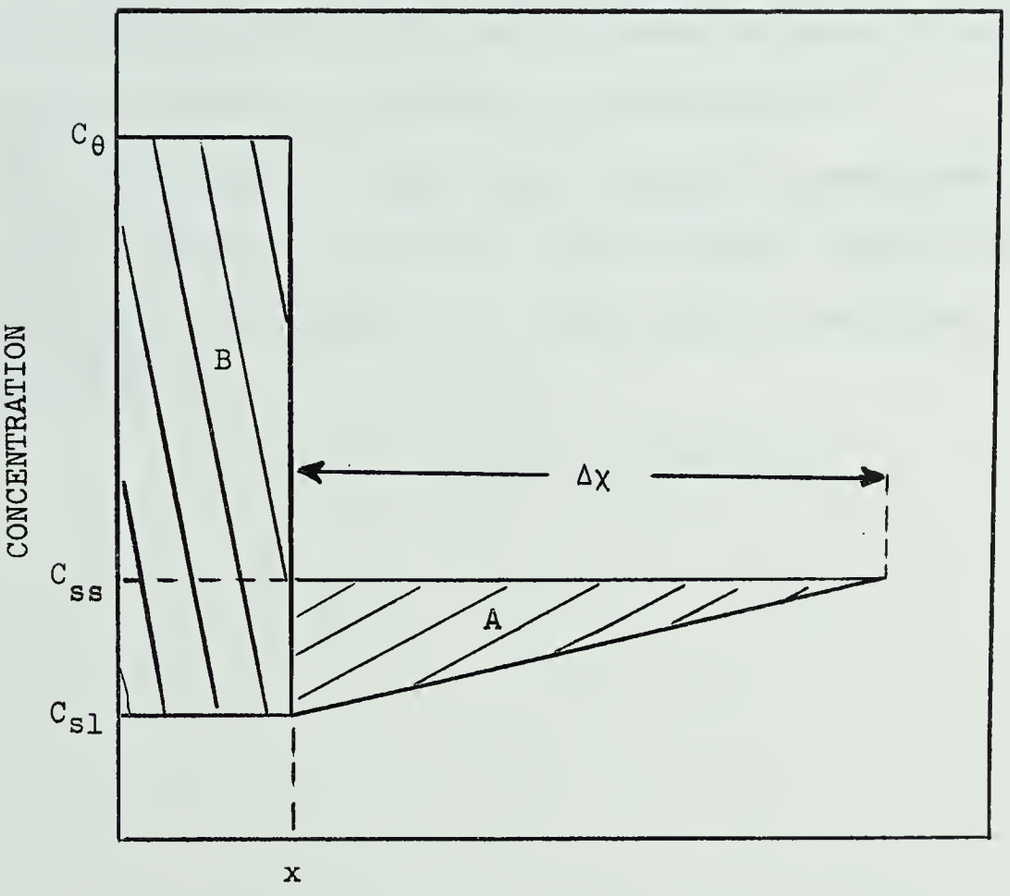

Figure 43. Approximate copper concentration profile in the region of the advancing precipitate/matrix boundary.

$$(C_\theta - C_{sl}).x = 1/2\ (C_{ss} - C_{sl}).\Delta x$$

$$(33 - 0.1).10^3 = 1/2\ (4 - 0.1).\Delta x$$

$$\Delta x.(1.95) = 32.9.\ 10^3$$

$$\Delta x = 16.9.\ 10^3\ \text{Å}$$

Thus the diffusion zone length is about $1.7.\ 10^{-4}$ cm. To a first approximation the diffusion width zone may be taken as the diameter of the specimen, 10^{-5} cm., and the l/w ratio is about 17, which is large enough to permit the formation of a Hall field.

NOTE:- The diffusion length zone, Δx, and the precipitate width or length along the x-direction, x, are related. Thus the l/w ratio will always be in the region of 17, even when the precipitate size differs from 10^{-5} cm.

ABBREVIATIONS

5X9s	This indicates a metal of 99.999% purity.
3X9s	This indicates a metal of 99.9% purity.
No-F	Identifies a no-field specimen.
A.M.( )	Ageing Method. Indicates the manner in which specimens were used in a particular experiment.
Chem.	Chemical.
Mech.	Mechanical. These terms are used with reference to polishing procedure.